5-2016

Alkaloids in e-cigarettes: their effects on cell growth and gene regulation

Maxwell H. Marlowe
University of Tennessee at Chattanooga, zct158@mocs.utc.edu

Alkaloids in E-cigarettes: Their Effects on Cell Growth and Gene Regulation

Maxwell H. Marlowe

Departmental Honors Thesis
The University of Tennessee at Chattanooga
Department of Biology, Geology, and Environmental Science

Project Director: Dr. Ethan A. Carver
Examination Date: April 4th, 2016

Members of Examination Committee:
Dr. Margaret J. Kovach
Dr. Gretchen E. Potts
Mrs. Beverly Kutz

Examining Committee Signatures:

_____
Project Director

_____
Department Examiner

_____
Department Examiner

_____
Liaison, Departmental Honors Committee

_____
Chairperson, University Departmental Honors Committee

Table of Contents

List of Figures

List of Tables

List of Equations

ABSTRACT

E-cigarettes have become increasingly popular in the past decade. They are marketed as smoking cessation aids. These products have not been well regulated or researched with respect to health concerns and safety issues. A number of toxic compounds have been discovered in refill solutions, and the long-term effects of e-cigarette use are still largely unknown. Nicotine is one of the primary alkaloids within e-cigarette refill solutions. Nevertheless, other tobacco alkaloids are present including; cotinine, myosmine and anabasine, even though these compounds are not disclosed on the packaging. This study uses known amounts of tobacco alkaloids, in an *in vitro* culture system, to test the effects of these chemicals on the growth of human lung cells. Cell viability was measured as a function of metabolic ATP activity, using the Cell-Titer Glo Luminescent assay. Preliminary results from single alkaloid trials indicate generally decreased cell growth in response to each of the aforementioned alkaloids, in comparison to a control. Changes in gene expression may be linked to the development of tobacco-related diseases in humans. To address this issue, we used qRT-PCR to analyze gene expression for multiple markers associated with diverse cellular functions: adhesion (*CEACAM6*, *CX3CL1*), immune response (*TLR4*, *CX3CL1*, *CEACAM6*), xenobiotic metabolism (*CYP1A1*, *AHR*, *ALDH3A1*), oxidative stress (*GPX2*, *ALDH3A1*), putative oncogenes (*PIR*, *CEACAM6*), and putative tumor suppressor genes (*SLIT1*). These markers were selected because their dysregulation is implicated in carcinogenesis and tumorigenesis. Expression of these markers will be compared between cells treated with the aforementioned alkaloids and control cultures. Our results show significant ($p<0.05$) differential expression of *TLR4*, *CEACAM6*, *ALDH3A1*, and *PIR* in response to alkaloid exposure. This project illustrates the need for more research on the contents and

physiological effects of refill solutions, and the requirement for better labeling and regulation of refill solutions.

ACKNOWLEDGMENTS

I would like to thank Dr. Ethan Carver for providing me the opportunity to participate in this project. You have been a constant source of support and motivation throughout this process, as well as during my difficult class loads, and my application processes to both internships and professional schools. I can genuinely say that I would not be where I am today without you. I would like to thank Dr. Margaret Kovach for the use of her lab, her reagents, and the inordinate amount of time she spent with me in order to instruct me and complete this project. You are an inspirational scientist, and I know I will be able to apply all you taught me to my future endeavors. I would like to thank Dr. Gretchen Potts for initiating this project, and providing the alkaloids used in this study. I would like to thank Professor Beverly Kutz for always offering me help, and making sure I had everything I needed to perform a valuable literature review.

GOALS and HYPOTHESIS

The goal of this project was to study the effects of alkaloids found in electronic cigarette (e-cig) refill solutions on normal gene expression and cell viability. Although there is an increasing popularity of the product, there is currently little available data regarding the potential consequences of electronic cigarettes on human health. There is a need for further investigation in the physiological effects of the major chemicals found in the cartridges, as well as the refill solutions themselves. The chemicals are vaporized and absorbed through the lungs where they enter the bloodstream and are distributed to various tissues and organs. Previous research in Dr. Carver's lab has shown decreased cell viability in cultures exposed to the four major alkaloids found in e-cig refill solutions, both singly and in combination with one another (Beavers, 2014). Based on this finding, we hypothesize that the cells are activating pathways that redirect energy from normal physiology and into stress responses. This research was designed to examine changes in gene expression and cell viability of a human lung cell line exposed to major chemical alkaloids found in e-cigarette refill solutions.

We exposed a human lung carcinoma cell line, CCL-185, to four major alkaloids that were extracted from the e-cigarette refill cartridges: nicotine, cotinine, myosamine, and anabasine. Cells were grown and maintained following protocols that allow for continued cell viability (Gibco). Cultured cells were exposed to individual alkaloids at dilutions of 1:10 and 1:1000 of the original 1mg/ml alkaloid stock, then the cell viability and gene regulation in the treated cells were compared to untreated control populations of cells. Cell viability was determined using a luminescent ATP assay, which correlates the amount of ATP present to the amount of metabolically active cells. Gene expression was

determined using reverse trancriptase PCR (RT-PCR). We chose candidate genes which are linked to tumorigenesis, oxidative stress, immune response, xenobiotic metabolism, and putative tumor suppressor genes and oncogenes. All the selected genes have shown differential expression in response to traditional cigarette smoke (Spira *et al*, 2004).

BACKGROUND INFORMATION

Cell Cultures

Cell cultures derive from cells that have been extracted from plant or animal tissues. When supplied with the proper nutrients, some of these cultures may be able to survive indefinitely. Cell culturing methodology allows each cell to function as an individual unit, which allows for control when studying cell growth, metabolism, or response to stimuli. Cell cultures provide a way to do certain tests *in vitro* that would be dangerous or unethical to perform on an *in vivo* system. Cultured cells are easily manipulated and are capable of showing varied responses to different stimuli (Brauze *et al,* 2014; Dasgupta *et al,* 2009). There are limitations to 2-D culture, in which the cells are plated on a solid substrate and form a monolayer. In the body, cells are suspended in a network of proteins called the extracellular matrix (ECM), and the cells are capable of communicating with one another, and with the ECM itself. There have been instances in which the reactions of cells in a 2-D system do not accurately portray the reactions of those cells in a 3-D system or *in vivo* (Abbot, 2003; Weaver *et al,* 1997). However, 2-D cultures are able to provide foundational research into the way cells will respond to stimuli such as oxidative stress and toxins, which will lead to further hypothesis and experimentation using more advanced techniques.

The American Tissue Culture Collection (ATCC) provides cell lines from many different tissues and organisms. We utilized the continuous-culture, human lung fibroblastic carcinoma cell line, CCL-185. This cell line is commonly used, and results generated using this study may be easily compared to other literature which utilizes this cell line. Since we are testing the cytotoxic effects of chemicals found in e-cigarette refill solutions it would be unethical to do these experiments on an *in vivo* system, thus the need for a 2-D culture. Cell culture will be a useful model for providing preliminary data relating to the effects of e-cigarettes on human health, and will provide guidance for further experimentation.

E-Cigarette

Since the early 2000s, the e-cig has become prevalent as a "safe" alternative to tobacco cigarettes (Caponnetto *et al*, 2012). Due to their lack of toxins arising from the combustion process, they may be safer than traditional cigarettes, though traditional cigarettes are a poor standard of health to be compared against. An increasing amount of young adults with no previous history of tobacco use have begun to smoke e-cigarettes, with 7.2% of high-schoolers, and 20.3% of middle-school e-cig users having never smoked a traditional cigarette (Carroll-Chapman *et al*, 2014). Despite their popularity, little is known about the long term physiological effects of e-cigs, or even the contents of the refill cartridges. Chromatographic analyses of refill solutions show nicotine, as well as other alkaloids: cotinine, myosmine, anabasine, β-Nicotyrine, and anatabine (Trehy *et al*, 2011; FDA, 2009; Murray, 2014). Analyses also show large discrepancies between the nicotine content marketed on the package, and the actual nicotine present in the

solution; in some cases, packages that were labeled as containing 0mg of nicotine actually showed up to 21mg of nicotine in the cartridge (Trehy *et al.* 2011). Measureable quantities of formaldehyde have been discovered in the vapor produced by e-cigarettes (Jensen *et al.* 2015). Brief inhalation of formaldehyde is associated with airway inflammation, and potential allergic reactions, while long term inhalation, such as that which may be obtained by habitual tobacco or e-cig use, is associated with increased asthma and cancer incidence (ATSDR, 2008).

A common marketing scheme among e-cigarette distributors consists of the client base being led to believe that the vapor produced by smoking e-cigarettes is solely water vapor. This marketing campaign made it initially acceptable to smoke e-cigarettes anywhere, including indoors, though many states are enacting regulations against this. Recent studies have shown that e-cigarettes reduce air quality, and emit substances that may be harmful toward humans. Increased amounts of nicotine, glycerine, 1,2-propanediol, aluminum, and polycyclic aromatic hydrocarbons (PAH) were detected in well-ventilated rooms in which e-cig use was taking place (Schober *et al*, 2014). While there is no side-stream smoke, as there is in traditional cigarette smoking, by-standers are exposed to exhaled vapor, which may carry these impurities in ultra-fine particles which are readily absorbed in lung tissue (Schober *et al*, 2014). The vapor also provides opportunity for third-hand exposure to vapor pollutants and nicotine. This occurs when the vapor settles on surfaces, and allows exposure via dermal contact, ingestion, or inhalation. The nicotine can react with oxidizing chemicals in the air and form carcinogenic nitrosamines (Goniewicz and Lee, 2015).

A recent study developed a murine model for e-cigarette smoking, which was shown to be comparable to human e-cigarette consumption based on correlations between serum cotinine levels. The study investigated whether or not the immune response of the mice was effected by 'smoking' e-cigarettes. The study examined mechanisms of bacterial and viral immunity by exposure to *Streptococcus pneumonia* and Influenza A, respectively. Mice exposed to e-cigarettes had decreased clearance of the bacterial species from their lungs, and showed reduced alveolar macrophage activity as compared to a control population. Mice exposed to the viral strain showed increased quantities of the virus in their lungs, and increased rates of disease-related mortality as compared to a control population. The authors hypothesize that some of the immunomodulatory responses are associated with nicotine exposure, which has been shown to be immunosuppressive, though the study did not investigate exposure to nicotine in isolation. The study also examined free radical content in e-cigarettes using electron paramagnetic resonance, which showed that e-cigarettes contain approximately 7×10^{11} free radical species per puff, which is less than the 1×10^{14} free radical species per puff in traditional tobacco smoke, but still enough to produce a heightened amount of oxidative stress (Sussan *et al*, 2015).

E-cigarettes are comprised of multiple units which work together to provide function (Figure 1). In all e-cigarettes there are six invariable main components: The mouthpiece, the atomizer, the microprocessor, the cartridge, the battery, and the fluid. The user inhales through the mouthpiece. The negative pressure triggers the atomizer, which vaporizes the E-liquid, which contains a humectant, such as propylene glycol, that allows it to be vaporized (Bahl *et al*, 2012). The refill cartridges contain the E-liquid and

the atomizer. These cartridges are simple to replace, and may be purchased in nearly 7,000 flavors (Allen *et al*, 2015), which may create appeal in youth populations and non-smokers (Callahan-Lyon, 2014). The chemical diacetyl was detected in a large proportion of the flavorings, this chemical has been linked to the disease bronchiolitis obliterans, "popcorn lung", which may require lung transplant in serious cases (Allen *et al*, 2015).

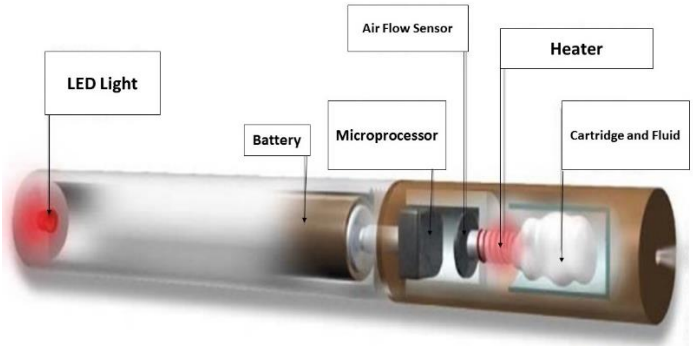

Figure 1: Functional Components of the Electronic Cigarette (e-cig)

(Adapted from http://ecigarettereviewed.com/about-e-cigs)

This project will evaluate effects of e-cigarette usage on a human cell culture system, which can be used to guide us on human health risks. Due to the novelty of the vaporized tobacco trend there has been little data published about the way in which e-cigarettes affect our body tissues or metabolic function. This project will provide insight into the responses that e-cigarettes elicit from the human body, and whether or not these responses are detrimental.

E-Cigarette Alkaloids

Nicotine

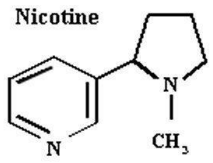

Figure 2: Chemical Structure of Nicotine

Nicotine (Figure 2) and its effects have undergone thorough research since the advent of the cigarette, and its increased use in modern society. Nicotine is a natural product of the tobacco plant, where it functions as an insecticide. It is the most abundant of the alkaloids found in the tobacco plant, making up approximately 95% percent of the total alkaloid content and 1.5% by weight of cigarette tobacco (Hukkanen *et al*¸2005). The nicotine content of conventional cigarettes is between 10-15mg (Kozlowski *et al*, 1998; Taghavi *et al*, 2012), but the content is variable in electronic cigarettes due to a lack of regulation by the FDA, and may range from 0-21.8mg in cartridges labelled as nicotine free, (Trehy *et al*, 2011). Nicotine is lipid-soluble, which allows it to cross the cell membrane, though this is influenced by the pH of the smoke. In more alkaline cigarettes, like those found in Europe, there is significant absorption of nicotine in the buccal mucosa of the mouth, but in more acidic cigarette smoke, like the ones found in America, the majority of the absorption occurs in the deep airway (Gori *et al*, 1986). Thus, the principle route of nicotine absorption occurs through the alveoli of the lung, which is aided by the large surface area of the alveoli (Yildiz, 2004). After inhalation of cigarette smoke, nicotine reaches the brain within 10-20 seconds producing rapid behavioral reinforcement by triggering the dopaminergic reward system (Benowitz *et al*,

2009). The smoker is able to titrate the amount of nicotine received through alterations in puff volume and frequency (Hukkanen *et al*, 2005; Farsalinos *et al*, 2015). Nicotine is also readily absorbed through the skin, which is an occupational hazard for farmers who work with wet tobacco leaves, which may cause Green Tobacco Sickness (McBride *et al*, 1998). There has also been an increased prevalence in toxic nicotine exposures through e-cigarette refill solutions with 5.9% of these exposures occurring through dermal contact (Chatham-Stephens, 2014).

Following the initial absorption, nicotine enters the bloodstream, and at a physiological pH it exists in a primarily ionized state. Nicotine has the highest affinity for the liver, spleen, kidneys, and lung, but with low affinity for adipose tissue. Nicotine also has a high affinity for brain tissue, with higher affinity in smokers than non-smokers due to increased nicotinic cholinergic receptors in the smoker's brain. Nicotine easily crosses the placental barrier and accumulates in amniotic fluid, as well as in breast milk (Hukkanen *et al*, 2005).

Average concentrations of nicotine in the venous blood of smokers are between 10-37ng/mL, and peak concentrations of nicotine are between 19-50ng/mL These numbers may vary based on the experience level of the smoker, or the mode of nicotine introduction, such as; cigarette, cigar, or chewing tobacco (Hukkanen *et al*, 2005). Arterial nicotine concentrations may be higher, reaching up to 100ng/mL (Benowitz *et al*, 2009). Blood levels in e-cig users vary depending on the generation of the device being used, and the experience level of the user. With first generation devices, using a cartridge with a mid-range nicotine content (18mg/mL), blood levels of nicotine peaked at

15.75ng/mL, and with a new generation e-cig the blood levels peaked at 23.47ng/mL (Farsalinos *et al,* 2014). Typically, 1mg of nicotine is absorbed per cigarette, though this may not be reflected in blood levels due to the short half-life and rapid distribution of nicotine (Hukkanen *et al*, 2005). Our study utilized nicotine concentrations which were 1µg/mL and 100µg/mL, which is higher than the physiological concentrations found in the blood, but may be more representative of the concentrations exposed to the lung epithelia prior to absorption. However, data regarding epithelial exposure to the alkaloids is limited, but this high and low range will provide a baseline of data regarding potentially dose-dependent effects of the alkaloids on lung cells.

Nicotine is metabolized in the liver. Six primary metabolites have been identified, but quantitatively and physiologically the most important is the lactam-derived metabolite, cotinine. In humans, 70-80% of nicotine is transformed to cotinine via a two-step mechanism, and then excreted in the urine (Benowitz *et al*, 2009). The primary step of this conversion is carried out by the cytochrome p-450 2A6 (CYP2A6) enzyme, which converts nicotine to a nicotine iminium ion (Yildiz, 2004), which is then converted to cotinine by an aldehyde oxidase. CYP2A6 shows extensive individual polymorphism and variation, which causes alteration in the metabolism and excretion of nicotine (Hukkanen *et al*, 2005).

Cotinine

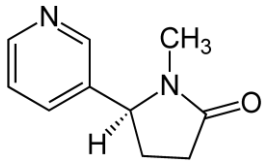

Figure 3: Chemical Structure of Cotinine

Cotinine (Figure 3) is the most abundant metabolite of nicotine, with 70-80% of nicotine being metabolized to cotinine (Benowitz *et al*, 2009). While nicotine is a natural product of the tobacco plant, it is thought that cotinine is produced through bacterial oxidation during tobacco processing (Benowitz *et al*, 2009). Cotinine can be further metabolized to several secondary metabolites (Figure 4), the most major of which are *trans*-3'-hydroxycotinine (33-40%) and cotinine glucuronide (12-17%). A large portion, between 10-15%, of cotinine is excreted completely unchanged (Benowitz *et al*, 2009). Physiologically, cotinine has no effect on mental acuity and no correlation to cardiovascular issues in humans (Hukkanen *et al*, 2005). High doses of cotinine have actually been shown to antagonize the effect of nicotine and aid in the alleviation of withdrawal symptoms (Hatsukami *et al*, 1998).

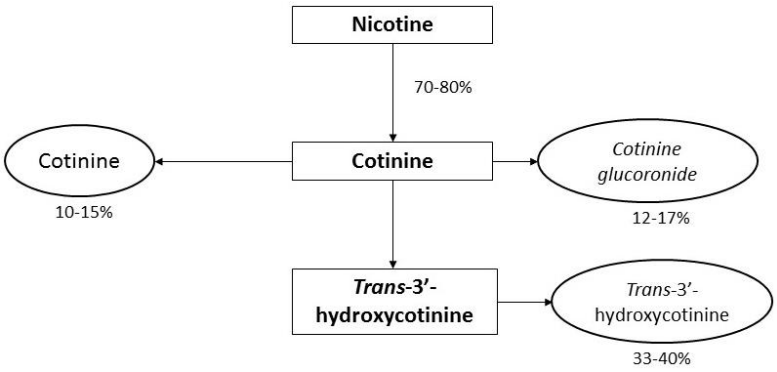

Figure 4: Quantitative Scheme of Nicotine Metabolism Showing Percentage of Alkaloids Appearing in Human Urine. This representation does not include all metabolites of nicotine or cotinine, but does include those with the most major presence in human urine (Adapted from Benowitz et al, *2009)*

Clearance is the term used to describe the volume of plasma cleared of a particular substance per unit time. Nicotine has a clearance rate of ~1200mL/min, while cotinine clearance is much slower, averaging ~45mL/min. Factors such as race, gender, diet and genetic variation in the CYP2A6 enzyme create variability in cotinine metabolism.

Nicotine has a relatively short half-life in biological fluids, approximately four hours, but cotinine has a half-life of approximately sixteen hours (CDC). Due to the persistence of cotinine in biological fluids, such as saliva and blood, as well as the large proportion of nicotine that is metabolically converted to cotinine, it is a useful biomarker for daily intake of nicotine. As shown in Figure 4, only 10-15% of cotinine is secreted unchanged. The main metabolites secreted through urine are *trans*-3'-hydroxycotinine and cotinine glucorinide. There are several factors that may cause variation in the efficacy of this mechanism. The aforementioned effects of race, gender, age and genetic variation all play a role in cotinine metabolism, and thus effect the usefulness of cotinine as a biomarker for nicotine intake (Benowitz *et al*, 2009; Benowitz, 1996).

Given that the majority of nicotine is converted to cotinine (Benowitz *et al*, 2009), and the high persistence of cotinine in biological fluids, the blood concentrations of cotinine are much higher than those of nicotine. Average blood concentrations of cotinine range from 200-350ng/mL, though it has been shown to be as high as 900ng/mL (Hukkanen *et al*, 2005). This *in vitro* tissue culture study utilized a low and high concentration of 1µg/mL to 100µg/mL, respectively, solubilized in the culture medium.

Though these concentrations are higher than physiological levels, they will provide us further understanding of potential dose-dependent effects of cotinine on a lung cell-line.

Anabasine

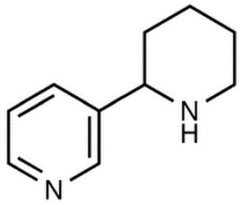

Figure 5: Chemical Structure of Anabasine

Anabasine (Figure 5) is a minor alkaloid that is produced by the tobacco plant as a natural insecticide. Nicotine makes up approximately 95% of the total alkaloid composition of the tobacco plant, while anabasine makes up ~0.3% (Armstrong *et al*, 1999). Unlike cotinine, anabasine is only found on the tobacco plant, it is not a nicotine metabolite, so presence of anabasine in biological fluids is indicative of active tobacco consumption (Yue *et al*, 2010). Comparatively, little research has been done regarding the physiological and psychological effects of anabasine. Anabasine has been shown to elicit similar addictive effects to nicotine, though at a lower potency than nicotine (Harris *et al*, 2015). However, it did not show effects on ambulatory behavior (Clemens *et al*, 2009). Anabasine has been implicated as a teratogen in livestock, leading to cleft palate and abnormalities related to prolonged skeletal muscle contraction in animals that were fed ground tobacco products (Lee *et al*, 2006).

Myosmine

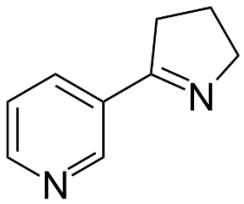

Figure 6: Chemical Structure of Myosmine

Similar to cotinine, myosmine (Figure 6) is believed to arise on the tobacco plant through bacterial oxidation during tobacco processing. Myosmine is also present in a variety of food products including nuts, cereals, cocoa, carrots, corn and cream (Simeonova *et al*, 2012; Benowitz *et al*, 2009). Its prevalence in food contributes to its presence in human toenails, saliva, plasma, and breast milk (Simeonova *et al*, 2012).

Myosmine metabolism has been shown to produce genotoxic and carcinogenic effects. Myosmine has five metabolites *in vivo*, the most prevalent of which are 3-pyridyl acetic acid (3-PAA) and keto acid (Glas *et al*, 2007). Under acidic conditions, myosmine can be directly converted to N'-nitrosonornicotine (NNN), which is implicated in the induction of esophageal tumors in smokers. When NNN is metabolically activated it leads to pirydyloxobutylating agents which bind to DNA, leading to mutagenic G to A conversions. Through peroxidation, myosmine can directly lead to molecules that form 4-hydroxy-1-(3-pyridyl)-1-butanone (HPB) producing DNA adducts, which have mutagenic effects on human cells (Vogt *et al*, 2006).

Like nicotine, myosmine is lipid soluble and passes easily through lipid membranes, thus following administration it is found in both intracellular and extracellular fluids. Myosmine shows high affinity for melanin, lachrymal and salivary

glands, stomach, and esophagus. Myosmine shows very rapid processing and excretion, appearing in the kidneys after several minutes (Glas *et al*, 2006).

Nicotine CNS Physiology

Nicotine has strong effects on the central nervous system, where it may cause locomotor stimulation, arousal, appetite suppression, and anxiety relief. Nicotine reaches the brain quickly, and crosses the blood-brain barrier with ease. Peak nicotine levels within the brain occur approximately 30 minutes after intravenous introduction, and within 30 seconds following cigarette smoking (Crooks *et al*, 1997; Hukkanen *et al*, 2005). Nicotine binds nicotinic acetylcholine receptors (nAChR) on the presynaptic terminals of cholinergic and dopaminergic neurons. These receptors are ligand gated channels, and nicotine and acetylcholine are both ligands. When a ligand binds, the channel is opened allowing an influx of cations and leading to depolarization of the neural membrane (Dani and De Biasi, 2001).

When nicotine first passes into the brain, nAChR is activated, causing an action potential, or nerve impulse, to travel the length of the axon and resulting in the release of dopamine. Dopamine is released in major reward centers, such as the nucleus accumbens and the ventral tegmental area (VTA), and the behaviors that allowed for this dopamine release are reinforced. Prolonged nicotine exposure then causes desensitization of nAChR, with nAChRs at active cholinergic synapses and high affinity nicotine receptors being more likely to desensitize than other receptor subsets. At these active cholinergic synapses, the receptors are exposed to high levels of acetylcholine (ACh) and nicotine

causing high levels of desensitization in these areas, and thus a decrease in normal information processing. The increased desensitization leads to a decreased rate of receptor turnover, and an increase in total receptors. When nicotine leaves the brain, the increased amount of desensitized receptors reactivate, leading to increased excitability of cholinergic neurons (Dani and De Biasi, 2001). There is a subnormal release of dopamine and other neurotransmitters, which leads to a state of irritability, inability to experience pleasure, and anxiety which has been dubbed "hedonic dysregulation", though this state can be quickly reversed by nicotine administration, which contributes to the difficulty conquering nicotine addictions (Benowitz, 2008).

In summary, nicotine and the other aforementioned alkaloids have generally negative impacts on human health. Nicotine has been shown to increase oxidative stress, increase respiratory inflammation (Jang *et al*, 2014), and causes behavioral adaptations associated with addiction (Benowitz, 2008). Myosmine has been shown to have genotoxic, carcinogenic and tumorigenic effects (Glas *et al*, 2007; Vogt *et al*, 2006). Anabasine has shown alterations to behavior similar to those in response to nicotine (Harris *et al*, 2015), and is speculated to be a teratogen in mammalian livestock (Lee *et al*, 2006). Cotinine has been shown to alleviate some of the effects of nicotine addiction and withdrawal symptoms (Hatsukami *et al*, 1998). The presence of these alkaloids in e-cigarette refill solutions are an indicator to negative effects on the health of e-cig users, and possibly those that are exposed to second and third-hand vapor from e-cigarettes.

Selected Candidate and Control Genes

Previous research in Dr. Carver's lab showed decreased cell viability in cells exposed to e-cigarette refill solutions, as well as those exposed to the alkaloids being investigated in this study (Beavers, 2014). It is likely the cells are diverting energy away from normal growth and metabolism and are instead allocating energy toward stress response pathways. In order to investigate this hypothesis, we selected a panel of nine candidate genes that would likely show abnormal expression if the cells were allocating energy in this manner. These genes are implicated in a diverse range of cellular processes such as oxidative stress, immune response, metabolism, adhesion, some of which have been characterized as putative oncogenes. We studied mRNA transcript expression of cells exposed to the various alkaloids, as compared to a control cell culture, using quantitative Real-Time PCR (qRT-PCR), in order to determine if these genes were differentially regulated in comparison to control cultures which were not exposed to the alkaloids.

CYPIA1 and AhR

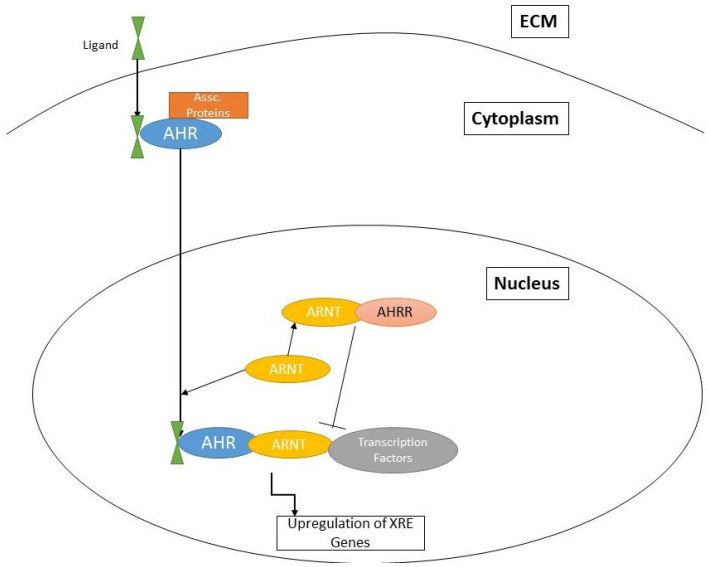

Figure 7: The molecular details of activation of Phase I and II XRE by the AhR/ARNT pathway (Adapted from Androutsopoulos *et al*, 2009)

The Cytochrome P450 (CYP) 1A1 is the major xenobiotic (drug metabolizing) member of the P450 superfamily in the lung. It has shown increased inducibility in the lungs of smokers in comparison with non-smokers and ex-smokers (Antilla, 1992). Its main function is the metabolism of polycyclic aromatic hydrocarbons (PAH) and dioxins such as 2,3,7,8-tetrachlorodibenzo-p-dioxin (TCDD), a key component of cigarette smoke. PAHs bind to the Aryl Hydrocarbon Receptor (AhR) (Figure 7), a cytoplasmic receptor protein, which translocates to the nucleus and upregulates a battery of xenobiotic-metabolizing enzymes (XME) (Brauze *et al*, 2014; Klein *et al*, 2010). The PAH only gains carcinogenicity after activation by Phase I xenobiotic-metabolizing enzymes, such as CYP1A1. Phase I of xenobiotic metabolism consists of modification of the ligand through hydrolysis, redox, or cyclization. The cytochrome P-450 molecules, such as

CYP1A1 or CYP1A2, attach an oxygen to the foreign molecule, making it more reactive and more susceptible to further metabolism by Phase II xenobiotic enzymes. These proteins function to transform the cytotoxic PAH to a more soluble and excretable form, but in the process they form metabolites that are able to bind DNA and form DNA adducts. The upregulation of responsive elements by AhR leads to altered metabolism and increased cytotoxicity and carcinogenesis (Brauze *et al*, 2014). The AhR signaling system operates on a negative feedback loop. The activation of CYP1A1 also activates the AhR regulator (AhRR), which prevents AhR from translocating to the nucleus (Klein *et al*, 2010; Lindahl, 1992). CYP1A1 inducibility is linked to lung cancer formation, but with variability in different ethnic populations (Chen *et al*, 2011). *CYP1A1* mRNA overexpression is common in the oral mucosa and airway of smokers vs non-smokers (Boyle *et al*, 2010). Our study will investigate transcript expression of *CYP1A1* in cells exposed to alkaloids found in e-cigarette refill solutions. Due to the role of CYP1A1 in processing reactive species, we hypothesize that transcript levels will be elevated in response to alkaloid exposure (Table 1). Investigating *AhR* in conjunction with *ALDH3A1* and *CYP1A1* expression levels may provide evidence as to whether or not any differential regulation of these genes is carried out under an AhR-dependent pathway.

ALDH3A1

Reactive aldehyde species can be generated through multiple endogenous and exogenous sources, including tobacco smoke and UV-radiation. Reactive aldehydes are similar to reactive oxygen species (ROS), except the aldehyde species last longer within the cell, and are membrane permeable so they may reach more distant targets. The

electrophilic character of the aldehyde carbonyl group confers reactivity to the aldehyde, which will interact with cellular nucleophiles such as proteins and nucleic acids (Lindahl, 1992). Reactive aldehydes cause DNA damage, enzyme inactivation, and often cell death. There are 19 genes in the Aldehyde Dehydrogenase (ALDH) superfamily, which detoxify both exogeous and endogenous aldehyde species by catalyzing their oxidation to carboxylic acids, using NADP+ as a coenzyme (Jang *et al*, 2014; Korkalainen *et al*, 1995).

ALDH3A1 is a $NADP^+$-dependent homodimer which is constitutively expressed in many tissues, including the cornea, lung, esophagus and stomach with nearly ubiquitous distribution through the cell. ALDH3A1 has exceptionally high concentration in the cornea, where it protects against aldehydes generated via exposure to UV-radiation (Black *et al*, 2012). Although ALDHs are often constitutive, there are forms that are induced by the presence of xenobiotics, which includes class III ALDHs, such as ALDH3A1. ALDH3A1 can be induced by the AhR signaling pathway as a Phase II XME (Lindahl, 1992), but its expression can also be induced through mechanisms independent of the AhR receptor (Korkalainen *et al*, 1995). Reactive aldehydes released by cigarette smoke can cause DNA interstrand crosslinks, which prevent the DNA helix from unwinding, thus preventing the effected sequence from undergoing replication or transcription. ALDH3A1, to a greater extent than other class III isozymes, attenuates cigarette smoke induced cytotoxicity through an AhR-dependent pathway (Jang *et al*, 2014). We hypothesize that the expression of *ALDH3A1* will be upregulated when exposed to the alkaloids present in e-cigarette refill solutions (Table 1).

GPX2

Glutathione peroxidase (GPX) is an enzyme that works to prevent oxidative stress by scavenging hydrogen peroxide and organic hydroperoxides in order to protect biomembranes and cellular components. GPX isoform 2 (GPX2) is the main inducible isoform of GPX in the lungs, and its transcript, as well as its protein expression increases in response to cigarette smoke (Singh *et al*, 2006). GPX facilitates the reduction of peroxides via the oxidation of glutathione (GSH) to glutathione disulfide (GSSG). Glutathione is an important redox couple in animal cells. It functions as an antioxidant via GPX, and also binds xenobiotics via the enzyme glutathione-s-transferase (Wu *et al*, 2004). Basal, as well as inducible expression of *GPX2* is dependent on the NF-E2-Related Factor (NFR2) transcription factor. In response to severely oxidizing ligands, NFR2 releases from repressor protein KEAP1 and binds the Antioxidant Response Element (ARE) and upregulates a battery of antioxidant proteins, including GPX2 in the lungs. *Nfr2*$^{-/-}$ null mice showed much higher levels of oxidative stress than their wild-type counterparts (Singh *et al*, 2006). Given its role in the oxidative stress response we would predict upregulation of GPX2 as a result of these experimental conditions (Table 1).

SLIT1

Members of the SLIT family, such as SLIT1, are extracellular matrix-secreted and membrane associated glycoproteins, which are the main ligands of the *roundabout* (ROBO) receptor. There are three isoforms of SLIT in mammals (SLIT 1-3), and there are homologues in many other organisms, including *Drosophila*, zebrafish, *Xenopus*,

chickens, and rats (Dickinson *et al*, 2004). SLIT proteins are produced in an inactive form, and must be cleaved in order to activate the ROBO receptor. The SLIT/ ROBO pathway plays an integral role in axonal guidance during embryogenesis, especially in the formation of commissural neurons, which have cell bodies on one side of the central nervous system (CNS) and extend axons to target cells on the opposite side of the CNS. The SLIT/ROBO complex forms a gradient which repels migrating axons away from the midline of the developing CNS and toward the opposing side (Dickinson *et al*, 2004; Avci *et al*, 2008; Ypsilanti *et al*, 2010).

Recently, the activities of the SLIT/ROBO pathway have been investigated in the context of tumorigenesis (Mehlen *et al*, 2011) and angiogenesis (Abdollahi *et al*, 2007; Mehlen *et al*, 2011). *ROBO1* and *SLIT1* have been implicated as potential pro-angiogenic genes during an analysis of the transcriptional network governing the angiogenic switch in pancreatic cancer, which is the shift in the balance between anti-angiogenic genes and pro-angiogenic genes. The instigation of angiogenesis is an important factor in tumorigenesis, because it allows the tumor to gain nutrients and growth factors required for growth and metastasis (Abdollahi *et al*, 2007; Mehlen *et al*, 2011). Based on the upregulation in *SLIT1* and *ROBO1* expression during tumorigenesis, we would predict that *SLIT1* will be overexpressed in response to the alkaloids found in e-cigarettes (Table 1). Though based on the complex networks and tissue associations required in angiogenesis and axonal guidance, it is difficult to predict whether *SLIT1* will show differential expression in a study utilizing 2-D cell culture.

PIR

Pirin is a putative nuclear transcriptional regulator, and therefore it is considered important to normal regulation of gene expression. Its N-terminus contains a single Fe^{2+} ion, which is evolutionarily conserved. This iron-binding domain is believed to confer biological activity, and the ability to bind with other transcription factors (Miyazaki *et al*, 2010).

Pirin (PIR) has been implicated in the process of tumor metastasis by aiding in the initiation of epithelial to mesenchymal cell transition (EMT). EMT is the process by which anchored epithelial cells lose their connection to the extracellular matrix and become motile mesenchymal cells. It is a common process during embryological development, and has recently been linked to tumor metastasis. Fixed tumor cells may undergo EMT and drift and implant in other regions of the body causing tumors to grow there as well. PIR functions to induce EMT by downregulating epithelial markers, such as E-cadherin and occludin, and upregulating mesenchymal markers N-cadherin, vimentin, and fibronectin (Komai *et al*, 2015). PIR is also implicated in apoptosis due to its association with nuclear factor κB (NF- κB), a highly regulated antiapoptotic transcription factor (Liu *et al*, 2013). *PIR* is highly upregulated during periods of oxidative stress and apoptosis. *PIR* mRNA expression was three-fold more in smokers than non-smokers, where its overexpression has been shown to induce apoptosis (Gelbman *et al*, 2007; Orzaez *et al*, 2001). The regulation of the interaction between PIR and NF- κB is poorly understood, but the apparent promotion of apoptotic mechanisms by PIR suggest that it plays an inhibitory role on NF- κB (Gelbman *et al*, 2007). We

hypothesize that *PIR* will be upregulated when exposed to alkaloids present in e-cigarettes (Table 1), due to the genes role in apoptosis and oxidative stress.

CX3CL1

CX3CL1 (also known as Fractalkine) is a chemokine, a type of chemoattractant cytokine. It is the only member of the CX3C class of chemokines. It exists as both a soluble and membrane bound form, the latter of which functions in cellular adhesion. In normal physiology chemokines have pleiotropic effects, largely influencing cellular migration during immune response, as well as angiogenesis, and mediation of the extra-cellular matrix. CX3CL1 and its receptor CX3CR1, are upregulated in several tumor types, including pancreatic and hepatocellular carcinomas (Li *et al*, 2010; Borsig *et al*, 2014). As with normal physiology, the role of chemokines is pleiotropic and far-reaching in cancer physiology as well. CX3CL1 functions as a tumor adhesion molecule, allowing tumor cells to communicate with stromal cells. Chemokines are regularly associated with immune function, and inflammation. The upregulation of the CX3CL1 protein is associated with the onset and maintenance of inflammation in liver disease. Chronic inflammation promotes persistent cellular proliferation, which in an inhospitable atmosphere, like that of inflammation or fibrosis, leads to increased probability of cancer cell formation. CX3CL1 has also been implicated in the process of angiogenesis, a process of paramount importance for tumor survival, by activating endothelial cells (Li *et al*, 2010). Due to its role in tumorigenesis we would predict increased expression of *CX3CL1* in this experiment (Table 1), though the results may be more pronounced if our experiment utilized primary cell cultures as opposed to a cancer cell line.

TLR4

The Toll-like Receptor 4 (TLR4) plays an important role in innate immunity. It is a pattern recognition receptor (PRR) that recognizes the lipopolysaccharide (LPS) and lipid A (LPA) present on the outer membrane of gram-negative bacteria. TLR4 is a membrane protein on cells of the innate immune system, as well as endothelial cells. When immune cells presenting the TLR4 receptor come into contact with LPS, they upregulate a battery of pro-inflammatory cytokines and chemokines. The pathway used by TLR4, as well as the intensity of the response, depends largely on the conformation of the LPS ligand (Stark *et al*, 2014). The alveolar macrophages (AM) in lungs of smokers' exhibit decreased cytokine production when stimulated by TLR4 agonists, though evidence indicates this occurs at a post-receptor level in the signaling cascade (Chen *et al*, 2007). Cotinine has been shown to reduce expression of ligand-stimulated TLR4 in cell culture (Bagaitkar *et al*, 2012). Based on the decreased immune response in smokers, we predict that cells will show decreased gene expression of *TLR4* (Table 1), especially those that are exposed to cotinine.

CEACAM6

Carcinoembryonic Antigen-like Cellular Adhesion Molecule 6 (CEACAM6) is a glycophosphotidylinositol-anchored membrane protein present in many primate tissues. It has a role in both innate and adaptive immunity, in which it mediates phagocytosis by adhering to proteins on the outer layer of gram negative bacterial and viral particles (Chapin *et al*, 2012). CEACAM6 exhibits homotypic binding with other CEA-presenting

cells, as well as heterotypic binding with integrin receptors, which allows its function in cell adhesion and migration. CEACAM6 expression is inversely correlated with cellular differentiation, and it is highly expressed in certain tumor types as compared to non-tumor tissue (Blumenthal *et al*, 2007; Kim *et al*, 2013). Abnormal expression CEACAM6 causes perturbation of specific integrins, which effects tissue architecture and regulation of cell differentiation. CEACAM6 exhibits inhibitory effects on anoikis, programmed cell death that occurs when a cell loses adherence to its substrate, which allows the onset of metastasis (Ordoñez *et al*, 2000). *CEACAM6* has increased mRNA in the airway of smokers as compared to non-smokers (Boyle *et al*, 2010; Spira *et al*, 2004). We would expect *CEACAM6* expression to increase when exposed to alkaloids found in e-cigarette refill solutions (Table 1), based on the role of the gene product in EMT and metastasis. Expression of this gene may be varied due to the cancer cell line, but comparison to the baseline expression of the control cultures may allow us to predict how this gene would be regulated in a primary culture.

Control Genes

Housekeeping genes code for proteins that provide essential maintenance or structural functions to the cell, and are therefore ubiquitous in all cells and tissues of the body and maintain relative stability regardless of the condition (Eisenberg and Levanon, 2013). We selected β-2-Macroglobulin (*B2M*) and β-actin for our housekeeping genes (Table 1). B2M is a protein that interacts with the major histocompatibility complex class one (MHCI), an immune complex that presents internally digested antigens and is present on every nucleated cell. β-actin is a cytoskeletal protein associated with motility, cell

structure, shape, and integrity. β-actin was used as an internal inter-plate control for the RT-PCR experiments, which will allow us to normalize the readings and compare relative gene expression in the genes under study.

Table 1: Predicted Differential Expression of Candidate Gene Biomarkers in Study

Gene	CYP1A1	TLR4	CEACAM6	GPX2	CX3CL1	PIR
Expression Variation	**Upregulate**	**Downregulate**	**Upregulate**	**Upregulate**	**Upregulate**	**Upregulate**
Gene	**SLIT1**	**AHR**	**ALDH3A1**		**B2M (CTRL)**	**B-Act (CTRL)**
Expression Variation	**Upregulate**	**Upregulate**	**Upregulate**		**Constant**	**Constant**

Materials and Methods

Tissue Culture Maintenance

The lung carcinoma cell line, CCL-185, was purchased from the American Tissue Culture Collection (ATCC). These cells were cultured in 75cm^3 Falcon Flasks and incubated at 37°C with 5% CO_2. Cells were grown in 12mL aliquots of DMEM High Glucose cell media supplemented with 10% Fetal Bovine Serum (FBS) and 1% penicillin-streptomycin solution. FBS provides growth factors that allow for normal cell growth and metabolism, and also provides inhibitors that halt the effects of trypsin during the cell passaging process. The penicillin-streptomycin solution prevents bacterial contamination of the eukaryotic cell culture. Cells were cultured until approximately 80% confluence within the flask.

Once cells reached confluency, media was removed and replaced with 3mL aliquots of 0.25% (w/v) trypsin supplemented with 2.23mM EDTA. Trypsin is a protease which cleaves peptides on the C-terminal side of lysine or arginine, which causes cells to lose adherence to the culture flask. Ethylenediaminetetraacetic acid (EDTA) chelates divalent cations such as Ca^{2+} and Mg^{2+}, which inhibit the protease function of trypsin. Cells were placed in the 37°C incubator for 5 minutes to assist in the proteolysis process. When the flasks were removed, the cells were suspended in solution. DMEM High Glucose supplemented with 10% FBS and 1% penicillin-streptomycin solution were added to the cell solution to bring the flask volume up to 24mL. A total of 12mL of this volume was removed and added to a new flask, effectively splitting the cell quantity of the original flask in half.

Chemical Set-up of Tobacco Alkaloid Exposure Plates

Cells were grown to confluence in 75cm^3 Falcon flasks. Upon reaching confluence, cells were trypsinized from flasks and cell counts were taken using a hemocytometer. Cells were counted in five sections of the hemocytometer, and the average cell count per square was determined. Each square contained 100nL. The average cell count per square was used to determine the average cell count per milliliter. The amount of cell stock required to seed 20,000 cells/mL was determined. Each experimental well was seeded with 20,000 cells in 1mL of solution, for consistency. Two dilutions of the alkaloids were prepared in culture media from the original 1mg/mL alkaloid stock: 1:10 and 1:1000, for final concentrations of 100µg/mL and 1µg/mL in the system, respectively. The molar concentrations varied depending on the molecular weight of the alkaloid (Table 2). Alkaloid stock was added directly to DMEM High Glucose,

supplemented with FBS and Penn/Strep. Cell stock was added directly to alkaloid dilutions and controls.

Table 2. Alkaloid Concentrations in Relation to Dilution Factors

	1:10 Dilution of 1mg/mL Stock		1:1000 Dilution of 1mg/mL Stock	
	Concentration (µg/mL)	Molar Concentration	Concentration (µg/mL)	Molar Concentration
Anabasine	100µg/mL	620 nmol/mL	1µg/mL	6.2 nmol/mL
Cotinine	100µg/mL	570 nmol/mL	1µg/mL	5.7 nmol/mL
Myosmine	100µg/mL	680 nmol/mL	1µg/mL	6.8 nmol/mL
Nicotine	100µg/mL	620 nmol/mL	1µg/mL	6.2 nmol/mL

For the plates that would be used for RNA extraction, each experimental condition was allocated an entire 12-well plate. The cells on the plates were pooled during the RNA extraction process, in order to ensure the maximum RNA yield. Each well contained 20,000 cells and 1mL of treated or control media.

Plates allocated to the Cell-titer luminescent assay each contained a control, and both dilutions of an alkaloid in triplicate. Each well contained 20,000 cells and 1mL of treated or control media.

Cell-Titer Glo Luminescent Viability Assay

The Cell-Titer Glo Luminescent Viability Assay is a high throughput method of determining the amount of cells in culture by detecting the amount of ATP present in the solution. The luminescence is produced by a thermostable luciferase reaction (Figure 8), which produces a “glow-type” reaction while simultaneously inhibiting endogenous ATPases, which would affect ATP measurements. The luciferin used in this assay is derived from the firefly *Photinus pennsylvanica*, which provides additional stability and sensitivity in comparison to the traditionally used luciferin derived from the firefly

species, *Photinus pyralis*. There is a 1:1 stoichiometric relationship between the firefly luciferin and moles of ATP used in the reaction, which allows for a direct correlation between ATP and luminescence.

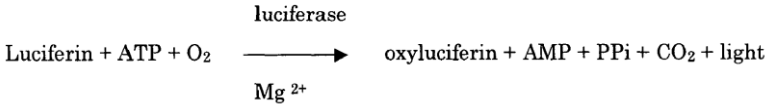

Figure 8: Chemical reaction utilized by the Cell-Glo Luminescent Assay. The firefly luciferin protein reacts with ATP produced by metabolically active cells in order to yield oxyluciferin and measurable light.

.

Cells were cultured on 12-well plates. Each plate contained a control in triplicate, which consisted of untreated DMEM High Glucose supplemented with 10% FBS and 1% Penicillin-Streptomycin solution. Two dilutions of an alkaloid (100µg/mL [Dil. 1] and 1µg/mL [Dil. 2]) were present, both in triplicate (Figure 9). Each plate was representative of a single time-point. A whole week was represented in the assay design. At each time point, the treated media and control media were each removed from the cultured cells, and replaced with 350µL of DMEM High Glucose that did not contain FBS or penicillin-streptomycin solution, because these supplements may interfere with the Cell-Glo buffer. A 350µL volume of the Cell-Glo media was added to the untreated media on the cultured

cells, which elicits an immediate color changing reaction. The plates were incubated on an orbital shaker for 10 minutes.

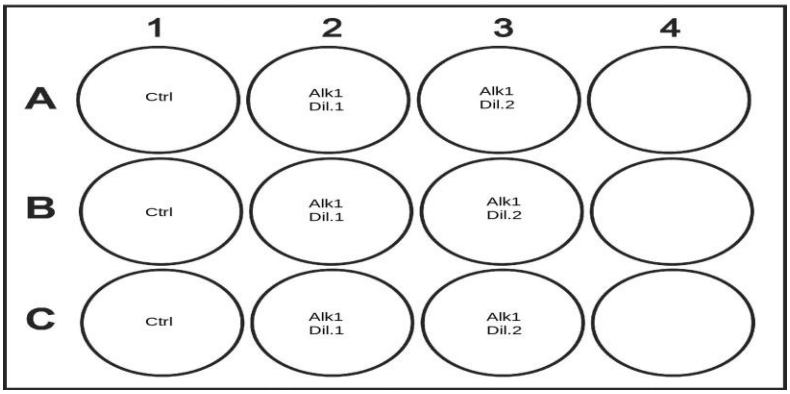

Figure 9: 12-Well Culture Plate Layout for the Cell-Glo Luciferase Assay. Dil. 1 represents the 100µg/mL dilution. Dil. 2 represents the 1µg/mL dilution.

Following incubation, 200µL of the Cell-Glo treated media was added to a reflective, white-walled 96-well plate. For a more quantitative assay, the experimental plates also contained a standard curve. The standard curve was prepared by creating solutions with known quantities of ATP and mixing with the Cell-Glo media (Figure 10). A 1µL volume of ATP stock was added to 5000µL of untreated DMEM High Glucose (2.00×10^{-10} mols ATP). A 2500µL volume of the solution containing 2.00×10^{-10} mols ATP was added to 2500µL of untreated DMEM High Glucose to create a solution containing 1.00×10^{-10} mols ATP. A 500µL volume of the solution containing 1.00×10^{-10} mols ATP was added to 500µL DMEM High Glucose to create a solution containing 5.00×10^{-11} mols of ATP. A 150µL volume of the solution containing 1.00×10^{-10} mols ATP was added to 1350µL of untreated media in order to make a solution containing 1.00×10^{-11} mols ATP. A 500µL volume of the solution containing 1.00×10^{-11} mols ATP was added to 500µL of untreated media to make a solution containing 5.00×10^{-12} mols ATP. Finally, 100µL of the solution containing 1.00×10^{-11} mols ATP was added to 900µL of untreated media to make a solution containing 1.00×10^{-12} mols ATP. A total volume of 100 µL of each

standard dilution, followed by 100 µL of Cell-Glo buffer, were added to individual wells of the opaque 96-well plate.

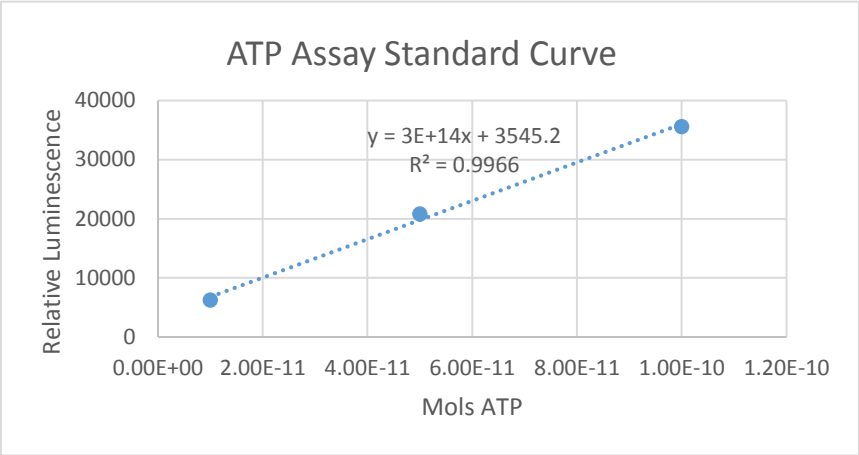

Figure 10: ATP Standard Curve generated for the Cell-Glo Luminescent Experiment

To prepare the experimental plates for luminescent reading, the treated or control media was removed from each well. It was replaced by 350µL of DMEM High Glucose that was not supplemented with FBS or Penn/Strep, in case those compounds would interfere with the action of Cell-Glo buffer. 350µL of the Cell-Glo buffer was then added to each well, causing an immediate color change reaction. The experimental plates containing the untreated media and the buffer, as well as the 96-well plate containing the standard, were incubated on an orbital shaker for 10 minutes, in order to ensure lysis of the cells and ATP release. Following the incubation 200µL of each experimental well was transferred to the 96-well plate. Each well from the 12-well plate was transferred to the 96-well plate in triplicate, the result being nine total wells per experimental condition for each alkaloid. The luminescence was read using a Biotek Synergy multi-mode plate reader. Results were analyzed in Excel™ (Microsoft, Redmond, Wa), details on the analytical methods used are found in the "Statistics" section of this thesis.

Real Time RT-PCR

Real-Time PCR (RT-PCR) allows for quantification of specific nucleic acid sequences by using fluorescent technology to monitor the amplification of the target sequence. One of the main uses of RT-PCR is studying gene expression levels by coupling with reverse transcription, which allows the researcher to quantitatively determine RNA transcript levels (Fraga *et al*, 2008).

There are three phases during a PCR amplification reaction: The exponential phase, the linear phase, and the plateau phase (Figure 11). During the exponential phase the PCR reaction is performing at or near 100%, so that the product doubles at each cycle. As the reaction progresses, the PCR components are steadily depleted, and the primer competes with the amplicon itself. As the reaction slows it enters the linear phase. There is no longer doubling of the product during each cycle, and the rate at which PCR components are depleted is highly variable, even amongst experimental replicates. The reaction will slow and stop during the plateau phase, due to depletion of substrate and product inhibition (Fraga *et al*, 2008).

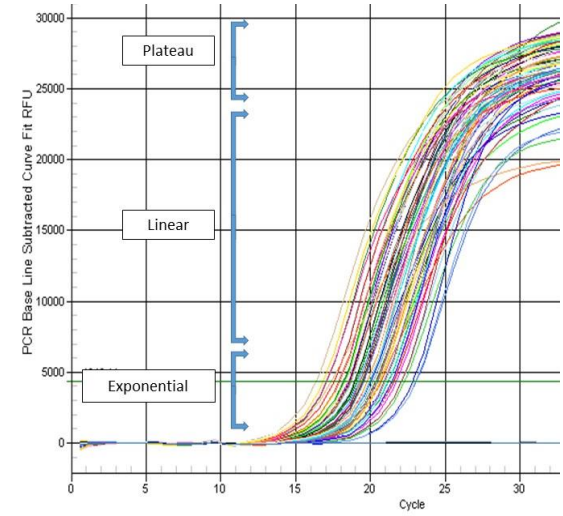

Figure 11: Plot of experimental PCR Reaction. x-axis: Cycle Number; y-Axis: Quantity of DNA. Three PCR phases are distinctly labeled: exponential, linear, and plateau.

Real Time RT-PCR measures amplicon production during each cycle of the reaction, and quantifies during the exponential phase when the reaction is occurring at maximum efficiency. There are several methods of doing this, the one utilized in this study utilizes the fluorescent dye SYBR Green. SYBR Green undergoes a 20-100 fold increase in fluorescence upon binding to double stranded DNA (Figure 12), and this increase was detected by the RT-PCR Thermocycler.

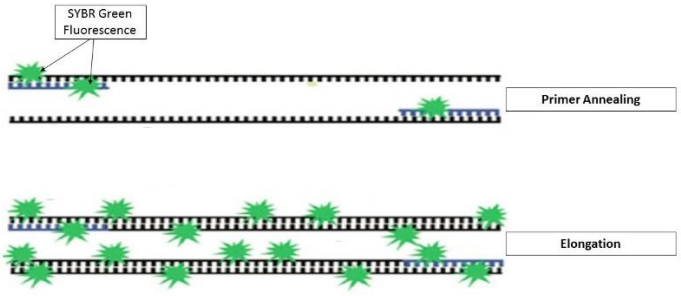

Figure 12: Illustration of SYBR Green intercalation during PCR amplification. The detector measures the fold increase when the dye is bound to the minor groove of dsDNA. This is used to quantify the DNA at the end of the elongation step (Adapted from Fraga et al, 2008).

Levels of candidate and control genes will be quantified using the relative standard curve method. Relative gene expression will be quantified as fold differences by using the $\Delta\Delta C_T$ method (Livak and Schmittgen, 2001). The cycle threshold (C_T) determines the level of fluorescence signal that is considered to be reliably over the background. The threshold must be set in a way that the product is detected while it is still in the exponential phase. The comparison of the C_T of different samples corresponds to differences in the starting amounts of the target sequence (Eqn 1), and thus difference in gene expression.

$$Fold\ Difference = 2^{C_{T1} - C_{T2}}$$

Eqn 1: Fold Difference in the Amount of Starting Target Expression

RNA Isolation

RNA was extracted from monolayers of cells grown in 12-well plates at two time points, 2-days post incubation and 7-days post incubation. Cells subjected to each experimental condition grown on the 12-well plates were pooled to provide a sufficient amount of cells to produce a useable quantity of total RNA. RNA was extracted using the RNeasy Mini Plus kit (Qiagen), following manufacturer's instructions. RNA integrity was tested by separation on RNase free 1.2% Agarose gel (Figure 13). Gels were checked for gDNA contamination and appropriate banding. RNA was quantified using Nanodrop.

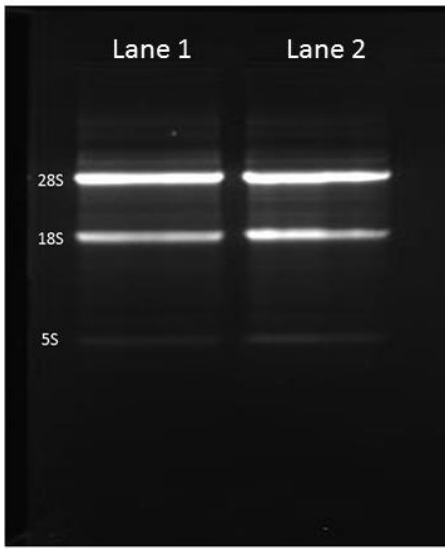

Figure 13: Evaluation of RNA integrity and purity by gel electrophoresis. RNA integrity is evaluated by monitoring the degradation of bands representing 28S, 18S, and 5S RNA. Purity of the RNA sample is indicated by the absence of contaminating high molecular weight, genomic DNA. Lanes 1 and 2 are representative RNA samples from untreated lung cell line, CCL-185. RNA was generated using the RNeasy Mini Plus Kit (Qiagen).

Two-Step Quantitative RT-PCR

Equivalent amounts of total RNA (1µg/µL) were reverse-transcribed to corresponding cDNA in a 20µL reaction mixture, using an iScript cDNA Synthesis kit. The cDNA synthesis conditions were as follows: 5 minutes of equilibration at 25°C, 30 minutes reverse transcription at 42°C, and 5 minutes of enzyme inactivation at 85°C. $1/20^{th}$ of the resulting cDNA was subjected to real time RT-PCR using the Real Master SYBR PCR Kit (Bio-Rad Laboratories, Hercules, CA). All qRT-PCR reactions were performed on the Biorad IQ5 Real-Time PCR detection system. Each plate intended for real time RT-PCR will test for one gene, and will contain the controls and both dilutions for all four alkaloids in triplicate for both time points, as well as a No Template Control (NTC), a No Primer Control (NPC), and an interplate control (IPC) (Figure 14). Plates of standards, ranging from 1.00×10^7 to 1.00×10^2 copy numbers, were run on RT-PCR prior to the experimental plates to determine efficiency of the primers.

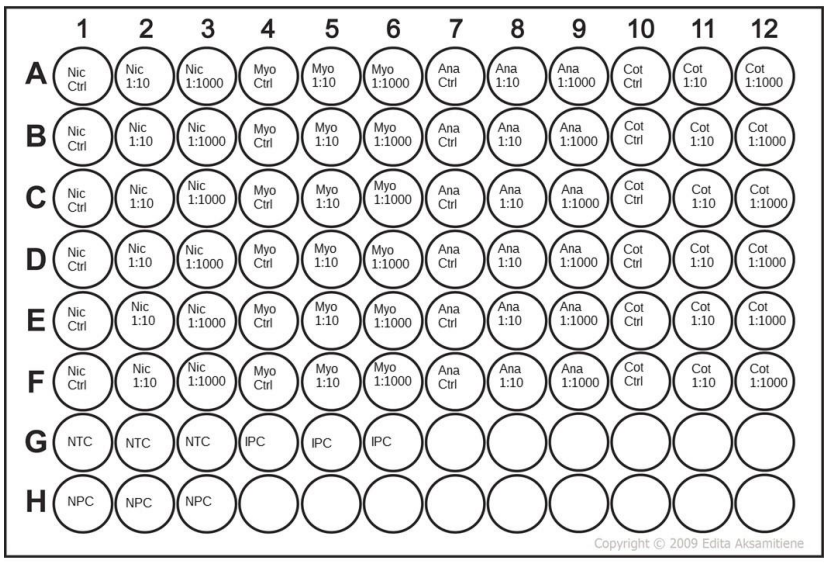

Figure 14: Layout of the 96-well RT-PCR experiment. Nic is representative of nicotine; myo is representative of myosmine; cot is representative of cotinine; ana is representative of anabasine. NTC is the abbreviation for the no template control; NPC is the abbreviation for the no primer control; IPC is the abbreviation for the inter-plate control.

Primer Design

Primers used for RT-PCR were designed using IDT Real-Time PCR SciTool, and were tested on untreated cDNA and run on 2% agarose gel to check for product specificity (Figure 15). Primer characteristics are described in Table 3.

Table 3: Primer details for each of the eight selected candidate genes, and the two control genes.

Primer Name	Sequence 5'-3'	Tm °C	Product (bp)	PCR Efficiency
ALDH3A1. FP	CCTTAAATACGTCCCCTCTTGG	62.7	96	93.1%
ALDH3A1. RP	TCGCTGATCTTGCTCATGG	60.2		
CEACAM6. FP	CTACAAGAGGTGGACAGAGAAG	62.8	149	92.5%
CEACAM6.RP	AATAGTGAGCTTGGCAGTGG	60.4		
CX3CL1. FP	CACCTTCTGCCATCTGACTG	62.4	130	95.8%
CX3CL1. RP	TGCCTGGTTCTGTGATAGTG	60.6		
GPX2. FP	GCTTCCCTTGCAACCAATTTG	60.6	139	125.8%
GPX2. RP	TTCTGCCCATTCACCTCAC	60.2		
PIR. FP	AGTAAGGATGGTGTGACATTG	60.8	135	97.7%
PIR. RP	AGGGATAGGTTGGGAATGTTTG	60.8		
SLIT1. FP	GACTGGCTACAAGGAACCG	62.3	149	99.5%
SLIT1. RP	TGGACAAGCAGAGATCACAC	60.4		
TLR4.FP	TGCGTGAGACCAGAAAGC	59.9	134	97.6%
TLR4.RP	TTAAAGCTCAGGTCCAGGTTC	55.6		
ACTB.FP	GGCCGCGGTGTACCAACACAGTGCTG	74.9	228	93.6%
ACTB.RP	CCCGGGGCCGTCACTCCTGCTTGCTG	74.9		
B2M. FP	ATGAGTATGCCTGCCGTGTGA	62.6	101	98.7%
B2M. RP	GGCATCTTCAAACCTCCATG	60.4		

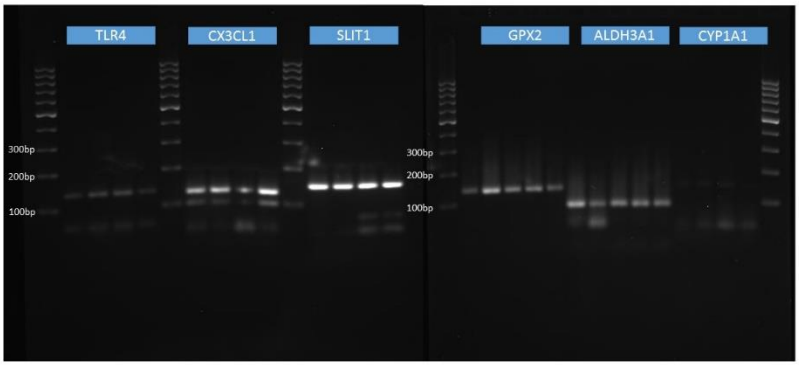

Figure 15: Evaluating primer specificity of gene targets by agarose gel electrophoresis against a 100bp ladder. All genes except CYP1A1 showing appropriate banding and densities adequate for gel extraction.

Results

Statistical Analysis

Cells were grown in triplicate for each experimental condition, and the control, on the 12 well plate, see Figure 9 for the plate layout used for this experiment. Cell lysates were produced in the 12 well plate and then each well was transferred into the reflective 96-well plate in triplicate. This produced nine wells total for each experimental condition. The readings produced were in relative luminescent units, which were converted to moles of ATP based on the results of the standard curve. The nine wells per experimental condition, in moles of ATP, were averaged, and the graphs were produced based on the arithmetic mean produced. The data was analyzed in Excel™. The standard deviation between replicates was determined, and t-tests were used to determine whether there were significant differences between experimental conditions and the control. Independent growth of the cell cultures allowed us to determine whether differences occurred due to random chance or due to an external factor, such as alkaloid exposure. Due to the independence of the data sets we used a two tailed, type 2 t-test. P-values less than 0.1 were used to highlight differences, while p-values less than 0.05 illustrate significant differences between data. At $p<0.05$, we can state with 95% certainty that the deviations in the data are not due to random chance. The graphs in the following sections were analyzed using these methods.

RT-PCR Experiments

Expression data was generated using the gene study tool on the Bio-rad IQ5 software. In this program the experimental genes' expression is normalized to our two reference genes, β-actin and β2M. Expression data for the experimental values were

compared to the experimental controls in order to obtain the percent difference values by using Equation 2.

$$\%\ Difference = \frac{(Experimental - Control)}{Control} \times 100\%$$

Eqn 2: Percent Difference to a Control

The gene expression study only delivers mean expression and mean C_T values, which are insufficient for significance testing, in which we utilized the t-test. We utilized the individual C_T values from each well of the experimental plate in order to obtain the triplicate values required for t-testing. However, these individual C_T values have not been normalized to the reference genes. In order to normalize the individual C_T for an experimental condition, we divided that C_T by the geometric mean of the mean C_T's of the reference genes for the corresponding experimental condition, as shown in Equation 3.

$$Normalized\ Expression\ for\ Individual\ Wells = \frac{C_{T\ (Exp)}}{\sqrt[n]{\bar{C}_{T(Ref1)} \times \bar{C}_{T(Ref2)} \ldots \times \bar{C}_{T(Refn)}}}$$

Eqn 3: Normalization of Individual C_T Values

The values produced by Equation 3, for each C_T value, were used for the two-tailed, type 2 t-test. P-values less than 0.1 were used to highlight differences, while p-values less than 0.05 illustrate significant differences between data. At $p<0.05$, we can state with 95% certainty that the deviations in the data are not due to random chance. The graphs in the following sections were analyzed using these methods.

Cell Proliferation

The following section addresses the results produced by the Cell-Titer Glo Luminescent Cell Viability assay. Previous research showed decreased cell viability in response to alkaloid exposure (Beavers, 2014), though that study utilized manual counting using hemocytometry. In this experiment, cells were grown in 12 well plates, in which they were exposed to the experimental or control conditions. On the time points being studied, the cells were exposed to the buffers associated with the assay kit, which lysed the cells and exposed the metabolic ATP that was previously within the cell to the luciferin contained within the buffer. The luciferin and the ATP react and create light, which was detectable using a multi-mode plate reader. The luminescence produced was then related back to the amount of metabolic ATP, and to the amount of metabolically active cells within the culture. This study sought to validate the results produced by Beavers (2014) utilizing a high-throughput, sensitive cell viability and proliferation assay, which is potentially less prone to human error than manual counting by hemocytometry.

Nicotine

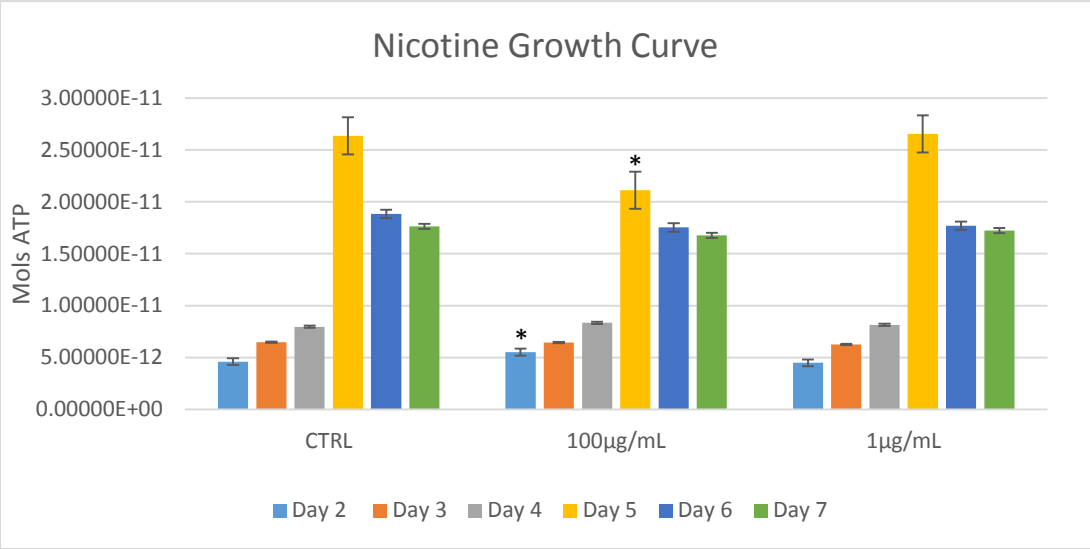

*Figure 16: Cell Viability in Response to Nicotine Exposure. * denotes p<0.05, # denotes p<0.1*

.

Figure 16 shows the results of the Cell-Titer Glo luminescent assay for cells exposed to nicotine dilutions over a period of seven days. The x-axis shows the dilution factor, as well as time, and the y-axis expresses moles of metabolically active ATP present in the cell lysate.

At day 2, nicotine shows increased growth in comparison to the control. Between days 4 and 5, during which the highest level of cellular proliferation took place, the growth of the cells decreased in comparison to the control.

The control cells showed a slow growth progression through day 4, with a sharp growth peak at day 5, where it increased from day 4 by 1.838 x 10^{-11} moles of ATP. Following this peak the control cells decreased in numbers, dropping by 7.528 x 10^{-11} moles of ATP. Days 6 and 7 showed a slow decrease in cell numbers. At a 100µg/mL dilution of the nicotine stock (1mg/mL) day 2 cell numbers were significantly greater

than those of the control by 9.162 x 10^{-13} moles of ATP. Days 3 and 4, as well as 6 and 7 closely mimicked the control culture, but day 5 was significantly decreased in comparison to the control culture by 5.252 x 10^{-11} moles of ATP. At a 1µg/mL dilution of nicotine stock (1mg/mL) cell proliferation closely followed the control curve, with no differences at $p<0.05$ or $p<0.1$.

We considered $p<0.05$ to indicate statistical significance, and $p<0.1$ to show difference. There were two data that showed statistical significance for our nicotine dilutions, and that was for our day 2 time-point and our day 5 time-point.

Cotinine

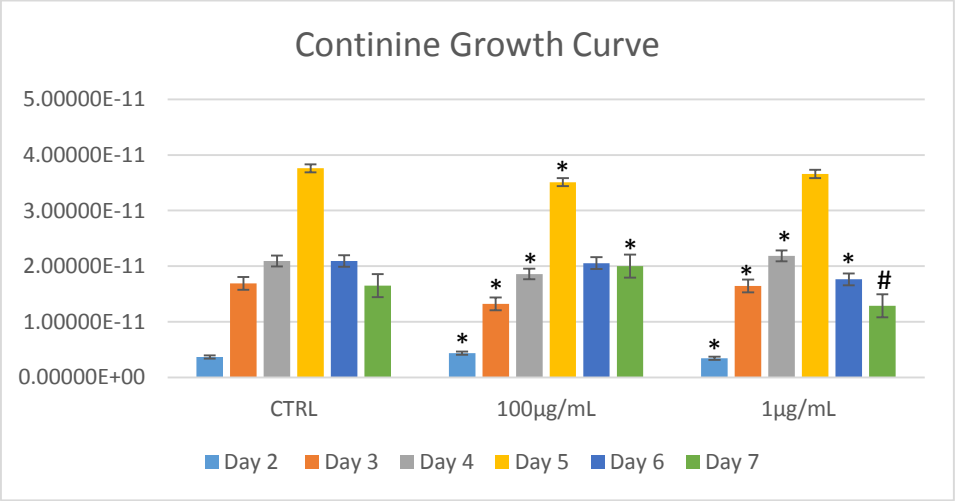

*Figure 17: Cell Viability in Response to Cotinine Exposure. * denotes $p<0.05$, # denotes $p<0.1$.*

Figure 17 shows the results of the Cell-Titer Glo luminescent assay for cells exposed to cotinine dilutions over a period of seven days. The x-axis shows the dilution factor, as well as time, and the y-axis expresses moles of metabolically active ATP present in the cell lysate.

The control cells showed a more dramatic growth progression between days 2 and 4 than the nicotine control cells, with generally higher numbers of cells overall. Like the nicotine cultures, the cell growth peaked at day 5, where it increased in the number of metabolically active cells by 1.666×10^{-11} moles of ATP. Following day 5 there was a sharp decline in cell numbers, back to the amount of ATP that was present in day 4. In general, the 100µg/mL and 1µg/mL dilutions of the cotinine stock (1mg/mL) showed greater effects in comparison to the control than the nicotine dilutions. The 100µg/mL dilution of the cotinine stock, similar to the 100µg/mL dilution of nicotine, surpassed the control culture on day 2, by 7.008×10^{-11} moles of ATP. Days 3, 4, and 5 of the 100µg/mL dilution were significantly decreased in comparison to the control culture. Day 3 was decreased in comparison to the control by 3.680×10^{-12} moles of ATP. Day 4 was lower by 2.323×10^{-12} moles of ATP. Day 5 was lower by 2.490×10^{-12} moles of ATP. Growth at day 7 of the 100µg/mL dilutions of cotinine surpassed that of the control culture by 3.533×10^{-12} moles of ATP.

The 1µg/mL dilution of cotinine also showed significant effects on cell growth, in comparison to the control cultures. Unlike the 100µg/mL dilutions of both nicotine and cotinine, the 1µg/mL dilution at day 2 showed decreased growth in comparison to the control, by 2.332×10^{-13} moles of ATP. Day 3 culture cell numbers were less than the control culture by 4.729×10^{-13} moles of ATP. Day 4 cell numbers significantly surpassed the control cultures by 9.488×10^{-13} moles of ATP. There was no significant difference in the cell numbers at the growth peak at day 5 for the 1µg/mL dilution. The drop between day 5 and day 6 was more dramatic than the control cultures, the difference being 3.314×10^{-12} moles of ATP between the day 6 for the control and 1µg/mL dilution.

Day 7 showed a difference that was significant at α=0.1, the 1µg/mL culture was decreased from the control culture by 3.611 x 10^{-12} moles of ATP.

We considered $p<0.05$ to indicate statistical significance, and $p<0.1$ to show difference. Both the 100µg/mL and 1µg/mL dilutions of the 1mg/mL cotinine stock showed significant differences at multiple time points. The 100µg/mL cotinine dilutions showed significance at α=0.05 for all time points except for day 6. Days 3 through 5 showed lesser cell numbers than the control, while days 2 and 7 surpassed the control for the respective time points. The 1µg/mL dilutions showed significance at α=0.05 for all days with the exceptions of days 5 and 7. Days 2, 3, and 6 were significantly decreased relative to the control, and day 4 was increased significantly. Day 7 showed a decrease that was significant at α=0.1.

Myosmine

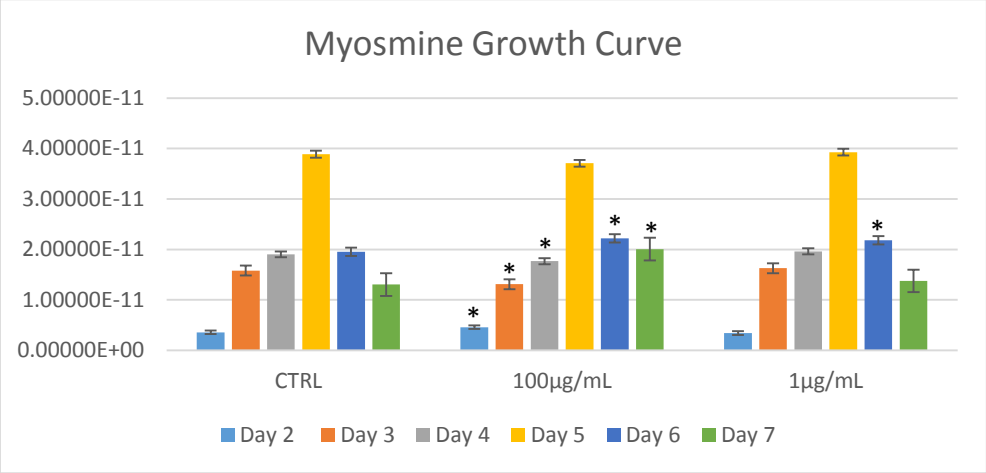

*Figure 18: Cell Viability in Response to Myosmine Exposure. * denotes $p<0.05$, and # denotes $p<0.1$.*

Figure 18 shows the results of the Cell-Titer Glo luminescent assay for cells exposed to myosmine dilutions over a period of seven days. The x-axis shows the dilution factor, as well as time, and the y-axis expresses moles of metabolically active ATP present in the cell lysate.

Similar to the cotinine control, the myosmine control showed a more pronounced increase in cells between days 2 and 3, followed by a slow upward progression between days 3 and 4. As with all of the other cultures, growth peaked at day 5, where it increased its number of metabolically active cells by 1.985×10^{-11} moles of ATP. Following the peak at day 5, there was a large drop off to approximately the same level as day 4 for day 6. There was a slow downward progression between days 6 and 7. The 100µg/mL dilutions of myosmine stock (1mg/mL) showed effects on cell growth that were statistically significant. Day 2 cultures exposed to the 100µg/mL dilutions surpassed the amount of metabolically active as evidenced by the 1.002×10^{-12} increase in moles of ATP. Days 3 and 4 showed a decrease in cell numbers as evidenced by a decrease in moles of ATP by 2.679×10^{-12} and 1.356×10^{-12}, respectively. Both days 6 and 7 showed increased cell numbers as illustrated by ATP increases of 2.645×10^{-12} moles and 7.025×10^{-12} moles, respectively. The 1µg/mL dilution mimicked the curve of the control culture closely, with the exception of the day 6 time-point, which showed an increase of 2.272×10^{-12} moles relative to the control culture.

We considered $p<0.05$ to indicate statistical significance, and $p<0.1$ to show difference. Both the 100µg/mL and 1µg/mL dilutions of the 1mg/mL myosmine stock showed significant differences to the control culture. The 100µg/mL cotinine dilutions

showed significance at α=0.05 for all time points except for day 5. Days 3 through 4 showed lesser cell numbers than the control, while days 2, 6, and 7 surpassed the control for the respective time points. The 1µg/mL dilutions showed significance at α=0.05 for day 6, which surpassed the cell growth of the control culture for the respective day.

Anabasine

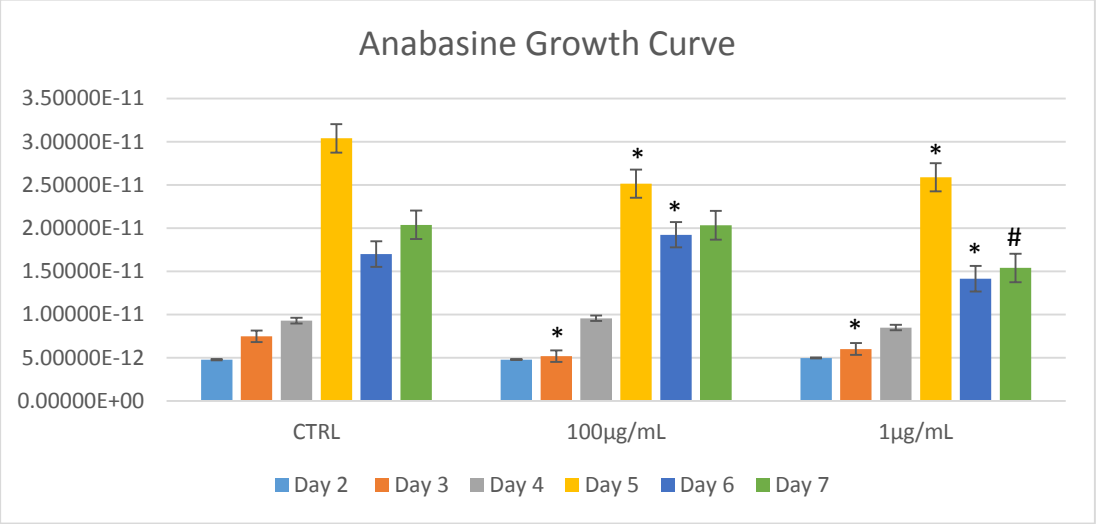

*Figure 19:Cell Viability in Response to Anabasine Exposure. * denotes p<0.05, and # denotes p<0.1.*

Figure 19 shows the results of the Cell-Titer Glo luminescent assay for cells exposed to anabasine dilutions over a period of seven days. The x-axis shows the dilution factor, as well as time, and the y-axis expresses moles of metabolically active ATP present in the cell lysate.

The control culture closely resembles the nicotine controls, in which there is a slow positive progression between days 2 and 4. There is a large spike between days 4 and 5, in which the quantity of metabolically active ATP increases by 2.11 x 10^{-11} moles. There is a pronounced decrease in cells between days 5 and 6, though it does not return to

the same level as it was on day 4, which the way the curve progressed in the cotinine and myosmine cultures. Unlike any of the other alkaloid control cultures, there is a positive progression between days 6 and 7, though given the temporal scope of the assay it is difficult to say whether the culture would have continued this progression into following days. The 100µg/mL dilution of the anabasine stock (1mg/mL) showed significant differences in cell numbers at multiple time points, in comparison to the control cultures. Day 3 and day 5 showed decreases in the number of metabolically active cells as evidenced by decreases in the amount of metabolic ATP by 2.291×10^{-12} and 5.248×10^{-12} moles. Day 6 for the 100µg/mL dilution surpassed the control cells, based on a relative increase in metabolic ATP by 2.239×10^{-12} moles.

The 1µg/mL dilution of the anabasine stock also showed significant differences relative to the control. Days 3, 5, and 6 all showed significant decreases in metabolically active cells as evidenced by decreases in metabolic ATP by 1.463×10^{-12}, 4.498×10^{-12}, and 2.860×10^{-12} moles, respectively. Day 7 showed a decrease that was significant at $\alpha=0.1$, in which the amount of metabolic ATP decreased by 4.997×10^{-12} moles.

We considered $p<0.05$ to indicate statistical significance, and $p<0.1$ to show difference. Both the 100µg/mL and 1µg/mL dilutions of the 1mg/mL anabasine stock showed significant differences to the control culture for multiple time points. The 100µg/mL cotinine dilutions showed significance at $\alpha=0.05$ for days 3, 5 and 6. Days 3 and 5 showed lesser cell numbers than the control, while days 6 surpassed the control for the respective time point. The 1µg/mL dilutions showed significance at $\alpha=0.05$ for days 3, 5, and 6, which were less than the cell numbers of the control culture for the respective

days. Day 7 showed a decrease of metabolic ATP that was significant at $\alpha=0.1$, which denotes a difference.

Gene Expression Results

This section will present the results of the gene expression study, which investigated differential expression of a battery of candidate genes in cells exposed to two dilutions of the alkaloid stock (1mg/mL). Previous research (Beavers, 2014), as well as the results produced by the Cell-Titer Glo assay in this study, demonstrated generally decreased cell viability in response to alkaloid exposure. We hypothesize that energy is being allocated away from normal growth and metabolism and into potential stress responses. To investigate this hypothesis, we utilized a two-step RT-PCR protocol to measure baseline mRNA transcript levels in cell cultures exposed to the alkaloid dilutions. Data is portrayed as percent difference in gene expression, as compared to a control culture.

Differential Gene Expression in Nicotine Treated Cell Cultures

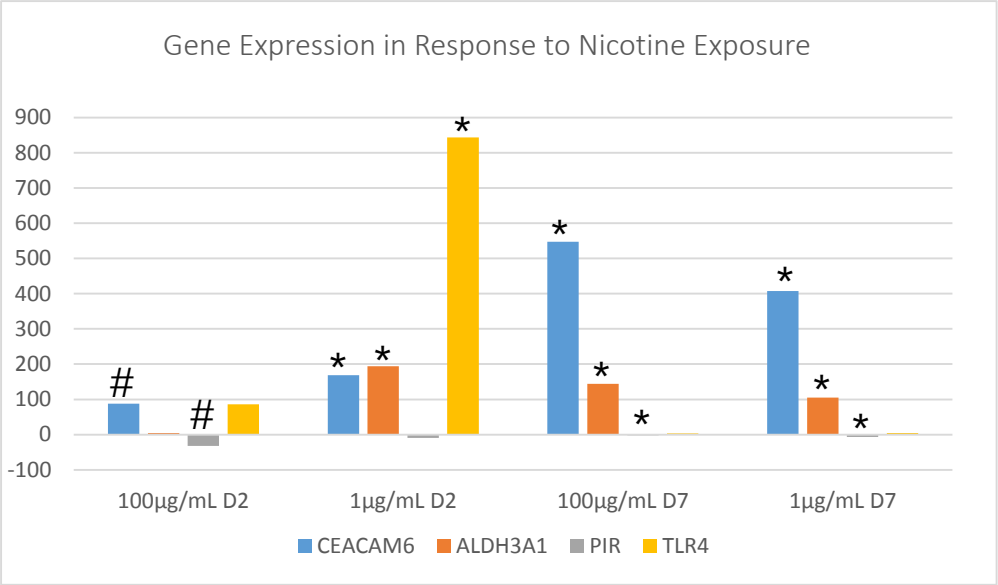

*Figure 20: Differential gene expression in cells exposed to nicotine dilutions. The graph shows data as percent difference to a control (y-axis). Positive values represent increased gene expression, and negative values represent decreased expression. * denotes $p<0.05$, # denotes $p<0.1$.*

Figure 20 shows differential gene expression as percent difference to control cultures, which were not exposed to nicotine. The y-axis represents percent difference, and the x-axis shows the time point (TP) and the dilution factor of the nicotine.

The 100µg/mL dilution of nicotine, two days past the initial seeding, showed differential expression of several genes. CEACAM6 showed increased gene expression that was significant at $\alpha=0.1$. CEACAM6 expression was increased by 87.8%, in comparison to the control culture. PIR showed reduced expression by -32.0%, which was significant at $\alpha=0.1$. The expression of TLR4 showed upregulation by 85.7%, and ALDH3A1 showed increased expression by 4.20%, though neither of these differences were deemed statistically significant using a student T-test.

The 1µg/mL dilution of nicotine, two days past the initial seeding, showed differential expression of each of the four genes. CEACAM6, ALDH3A1, and TLR4 showed significantly ($p<0.05$) increased expression, by 168.2%, 194.1%, and 843.6% respectively. PIR showed reduced expression by -9.89%, though this difference was not deemed statistically significant.

The 100µg/mL dilution of nicotine, seven days past the initial seeding, showed differential expression of each of the four genes, three of which showing significant differences at $\alpha=0.05$. CEACAM6 and ALDH3A1 showed significantly ($p<0.05$) increased expression by 547.2% and 144.5%, respectively. PIR showed significant downregulation of gene expression by -1.77%. TLR4 showed a 3.57% increase in gene expression, which was not shown to be significant using a student T-test.

The 1µg/mL dilution of nicotine, seven days past the initial seeding, showed significant differences in gene expression in three of the four genes. CEACAM6 and ALDH3A1 showed upregulation of gene expression by 407.3% and 105.3%, respectively, both of which were significant at $\alpha=0.05$. PIR showed significantly ($p<0.05$) reduced expression by -6.51%.

In summary of the effects of nicotine, CEACAM6 and PIR showed differential expression that was significant at $\alpha=0.1$, for the 100µg/mL dilution of nicotine on the day 2 time-point. The gene expression of CEACAM6 and ALDH3A1 showed statistically significant ($p<0.05$) upregulation for the 1µg/mL nicotine dilution for both time-points, as well as the 100µg/mL dilution for the day 7 time-point. PIR showed significant ($p<0.05$) downregulation of gene expression for both of the day 7 time-points.

Differential Gene Expression in Myosmine Treated Cell Cultures

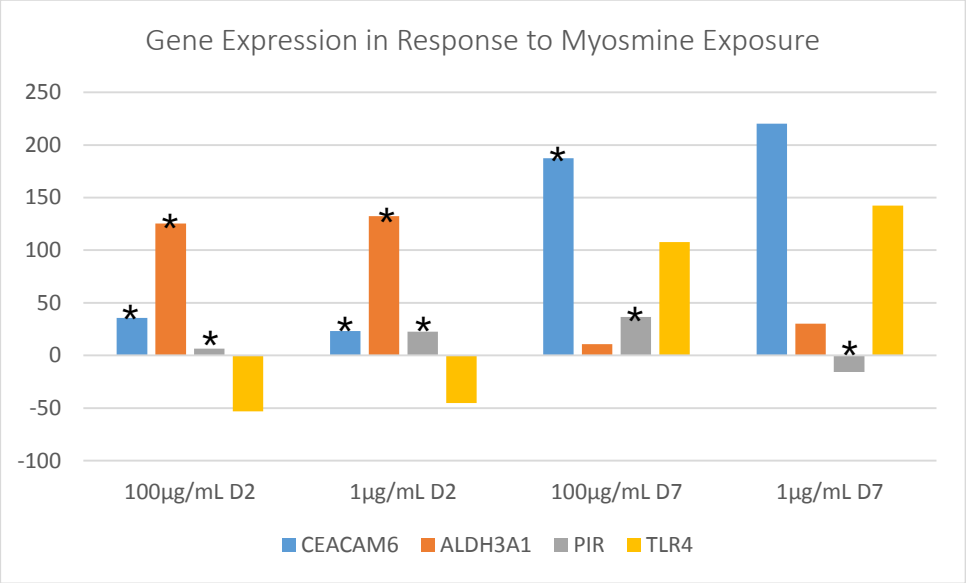

*Figure 21: Differential gene expression in cells exposed to myosmine dilutions. The graph shows data as percent difference to a control. Positive values represent increased gene expression, and negative values represent decreased expression. * denotes p<0.05, # denotes p<0.1.*

Figure 21 shows differential gene expression as percent difference to control cultures which were not exposed to myosmine. The y-axis represents percent difference, and the x-axis shows the time point (TP) and the dilution factor of the nicotine.

The 100µg/mL dilution for the day 2 time-point showed differential expression of all genes, three of which, CEACAM6, PIR, and ALDH3A1 showed differences which were significant at $\alpha=0.05$. CEACAM6, PIR, and ALDH3A1 showed significantly increased expression by 35.6%, 6.63%, and 125.52%, respectively. TLR4 showed expression which was reduced by –53.0%. TLR4 showed no significant difference at $\alpha=0.05$ or $\alpha=0.1$.

The 1µg/mL dilution for the day 2 time-point also showed differential expression of CEACAM6, ALDH3A1, and PIR, all of which were statistically significant. CEACAM6, PIR and ALDH3A1 showed significant upregulation of gene expression by 23.1%, 22.5%, and 132.3%, respectively. TLR4 showed reduced expression by 45.2%, though not at a level that was deemed significant at $\alpha=0.05$ or $\alpha=0.1$.

The 100µg/mL dilution for the day 7 time-point showed upregulation of gene expression for all four genes, three of which showed differences at $\alpha=0.05$. CEACAM6 and PIR showed significantly ($p<0.05$) increased expression by 187.4% and 36.6%, respectively. TLR4 and ALDH3A1 showed increased expression by 107.9% and 10.82%, but did not show significance at $\alpha=0.05$ or $\alpha=0.1$.

The 1µg/mL dilution for the day 7 time-point showed significant differential expression of PIR. The expression of PIR was significantly decreased by -15.8%. The expression of CEACAM6, TLR4, and ALDH3A1 was increased by 220.26%, 142.3%, and 30.2%, respectively, although none of these differences showed significance at $\alpha=0.05$ or $\alpha=0.1$.

In summary of the effects of myosmine, CEACAM6 showed significant ($p<0.05$) upregulation of gene expression for all dilutions and time points, with the exception of the 1µg/mL dilution on the day 7 time-point. PIR showed significantly increased expression for the 100µg/mL dilution at the day 2 and day 7 time-points, as well as the 1µg/mL dilution at the day 2 time-point. PIR showed significant downregulation of gene expression for the 1µg/mL dilution at the day 7 time-point. ALDH3A1 showed significantly increased expression for both dilutions on the day 2 time-point, and

insignificant upregulation of gene expression for both dilutions at the day 7 time-point. TLR4 showed no statistically significant differential expression for any dilution or time point.

Differential Gene Expression in Anabasine Treated Cell Cultures

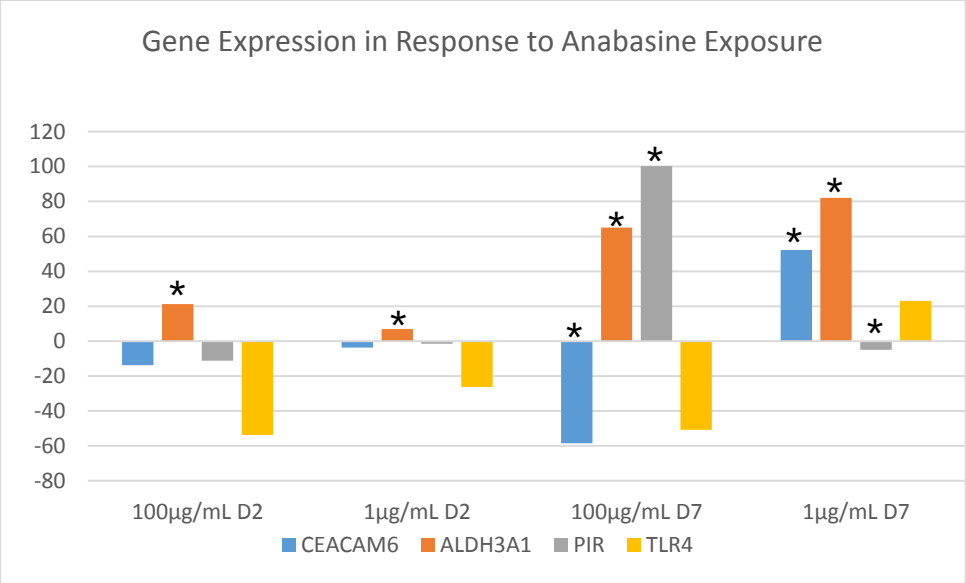

*Figure 22: Differential gene expression in cells exposed to anabasine dilutions. The graph shows data as percent difference to a control. Positive values represent increased gene expression, and negative values represent decreased expression. * denotes $p<0.05$, # denotes $p<0.1$*

Figure 22 shows differential gene expression as percent difference to control cultures which were not exposed to anabasine. The y-axis represents percent difference, and the x-axis shows the time point (TP) and the dilution factor of the anabasine stock (1mg/mL).

The 100µg/mL anabasine dilution for the day 2 time-point showed differential expression in all detectable genes, but only ALDH3A1 showed a difference to the control that was significant at $\alpha=0.05$. The expression of ALDH3A1 was significantly ($p<0.05$)

increased by 21.27%. The expression of CEACAM6, TLR4, and PIR was reduced by -13.7%, -53.7%, and -11.3%, respectively, though these differences were not deemed statistically significant using a student t-test.

The 1µg/mL dilution for the day 2 time-point showed significantly ($p<0.05$) reduced expression in PIR by -1.42%. No other genes showed significant differential expression for this dilution and time point.

The 100µg/mL dilution for the day 7 time-point showed differential expression in three of the four genes at a level that was significant $\alpha=0.05$. CEACAM6 showed statistically significant ($p<0.05$) downregulation of gene expression by -58.5% in respect to the control cultures. ALDH3A1 and PIR showed significantly increased expression by 64.98% and 100.3%, respectively. TLR4 showed statistically insignificant downregulation of gene expression by -50.73%.

The 1µg/mL dilution for the day 7 time-point showed statistically significant ($p<0.05$) differential expression for three of the four detectable genes. CEACAM6 and ALDH3A1 showed statistically significant ($p<0.05$) upregulation of gene expression by 52.2% and 82.0%, respectively. PIR showed significantly reduced expression in comparison to the control by -4.99%. TLR4 showed insignificant upregulation of gene expression by 23.08%.

PIR showed significant downregulation of gene expression at the 100µg/mL dilution for the day 2 time-point, as well as the 1µg/mL dilution for the day 7 time-point. PIR showed statistically significant upregulation of gene expression at the 100µg/mL

dilution for the day 7 time-point. The expression of CEACAM6 was significantly decreased at the 100µg/mL dilution for the day 7 time-point, and significantly increased for the 1µg/mL dilution of the same time point. ALDH3A1 showed significant upregulation of gene expression in cells treated with both dilutions at the day 7 time-point, as well as the 100µg/mL dilution on the day 2 time-point. TLR4 showed differential expression for each condition and time point, but none that were deemed significant using the student t-test.

Differential Gene Expression in Cotinine Treated Cell Cultures

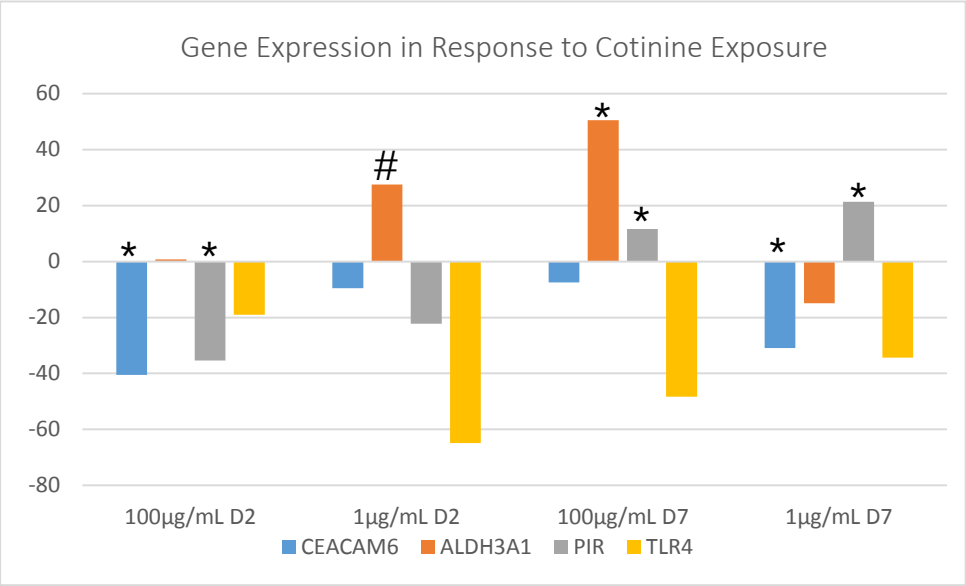

*Figure 23.Differential gene expression in cells exposed to cotinine dilutions. The graph shows data as percent difference to a control. Positive values represent increased gene expression, and negative values represent decreased expression. * denotes p<0.05, # denotes p<0.1*

Figure 23 shows differential gene expression as percent difference to control cultures which were not exposed to cotinine. The y-axis represents percent difference, and the x-axis shows the time point and the dilution factor of the cotinine stock (1mg/mL).

The 100µg/mL dilution for the day 2 time-point showed statistically significant differential expression in three of the four genes. CEACAM6 and PIR showed significantly ($p<0.05$) reduced expression, in comparison to control cultures, by -40.5% and -35.4%, respectively. ALDH3A1 showed increased expression by 0.789%, and TLR4 showed decreased expression by -18.99%, though neither were deemed statistically significant using the student t-test.

The 1µg/mL dilution for the day 2 time-point showed a marginally significant ($p<0.1$) increase in expression for ALDH3A1. Expression of ALDH3A1 was increased by 27.55%, in comparison to the control. The expression of CEACAM6, PIR, and TLR4 was decreased by -9.59%, -22.19%, and -64.83%, respectively. None of these values were deemed significant at $\alpha=0.05$ or $\alpha=0.1$.

The 100µg/mL dilution for the day 7 time-point showed significant differential expression for three of the four genes. CEACAM6 showed significantly decreased expression by -7.51%, in comparison to the control culture. PIR and ALDH3A1 showed significantly upregulated gene expression by 11.59% and 50.52%, respectively. TLR4 showed reduced expression by –48.3%, though this was not deemed significant at $\alpha=0.05$ or $\alpha=0.1$.

The 1µg/mL dilution for the day 7 time-point showed significant differential expression for PIR, which was significantly ($p<0.05$) upregulated by 21.32%. ALDH3A1 and TLR4 exhibited decreased expression by -14.90% and -34.30%, respectively, though not a level that was significant at $\alpha=0.05$ or $\alpha=0.1$.

CEACAM6 showed decreased expression for all dilutions and time points, though only the 100µg/mL dilution for both time points exhibited reduced expression at a level that was statistically significant ($p<0.05$). ALDH3A1 showed increased expression for the 1µg/mL dilutions for the day 2 time-point at a level that was significant at $\alpha=0.1$, and significant upregulation of gene expression ($p<0.05$) for the 100µg/mL dilution at the day 7 time-point. PIR showed significant differential expression for all dilutions and time points, with the exception of the 1µg/mL dilution during the day 2 time-point. It exhibited decreased expression for the day 2 time-points, and increased expression for the day 7 time-points. TLR4 showed decreased expression for all points, though not at a level that was significant at $\alpha=0.05$ or $\alpha=0.1$.

Discussion

This section will discuss the implications of results produced by the cell viability and RT-PCR experiments. The results will be discussed in the context of how they conform to the hypotheses, as well as their potential effects on the health of the cell and the human body as a whole.

Cell-Titer Glo Luminescent Cell Proliferation Assay

This assay was used as a high-throughput and accurate method for characterizing cell culture growth. We performed the week long assay three times total. The first time we only examined cell growth on day 2 and day 7, but we felt like we were unable to accurately convey the growth effects of the alkaloid using only two time points. The second time we examined cell growth daily, for a period of seven days, in order to insure a comprehensive perspective on the cells growth curve. However, due to a malfunction in

the culturing process, the cultures treated with a 100µg/mL dilution of the myosmine failed to adhere to the 12-well culture plate, so myosmine was unable to be included in the investigation. We decided to repeat the experiment to insure validity and get readings for cells cultured in the myosmine dilutions. All cells were successfully cultured, and upon visual inspection appeared in better health than those of the previous assays, so this assay bears the weight of scrutiny, although the other assays are not out of consideration. However, during the period of the third seven-day assay we ran out of reflective, white-walled 96-well plates, so we were forced to reuse one. Between runs of the assay the plate was rinsed with DI water, lab quality soap, followed by DI water and 70% alcohol, and then air-dried. The triplicates for each well remained close, and the standard showed little variance between plates, indicating that this process did not interfere with reproducibility of the assay. The standard deviation between triplicates was lower than that of the second set of assays performed. This being said, it is my belief that the assay should be repeated in future studies to ensure validity.

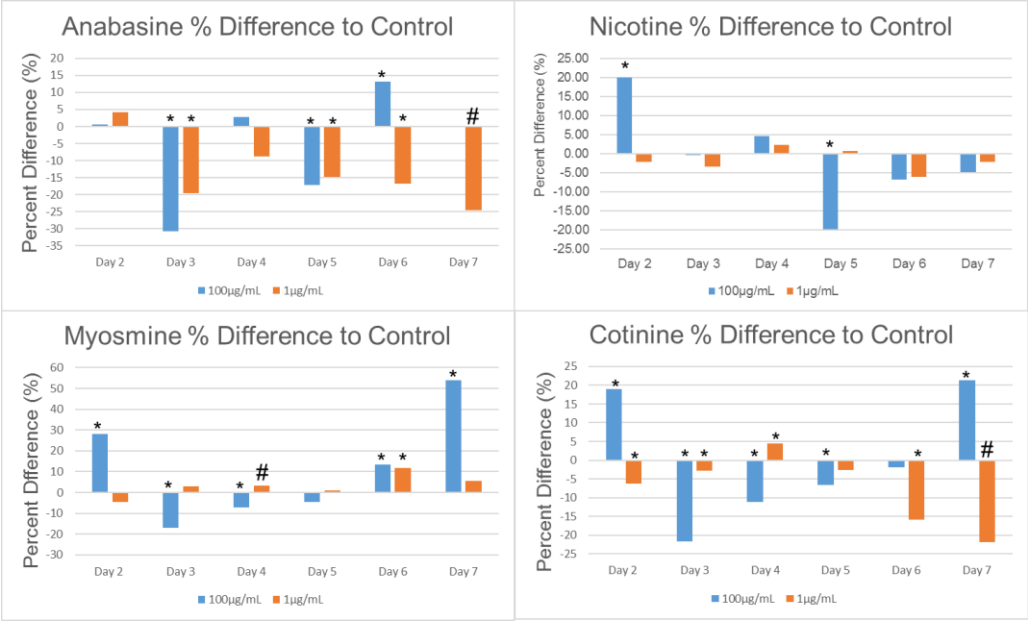

*Figure 24: Alkaloid treated cells percent difference in cell proliferation, as compared to control cultures. Negative values represent decreased growth, while positive values represent growth that surpassed the control cultures. * denoted $p<0.05$, and # represents $p<0.1$.*

Interestingly, of the four alkaloids, nicotine showed the least effect on cell growth and proliferation. Significant differences ($p<0.05$) were only observed at the more concentrated 100µg/mL dilutions, and only on days 2 and 5 of the assay. Day 2 showed a 19.89% increase compared to the control culture, while day 5 showed a 19.92 % decrease compared to the control (Figure 24).

Cotinine showed the greatest effect on the cell cultures. All of the time points for the 100µg/mL dilution, with the exception of day 6, showed significant differences at $\alpha=0.05$. Days 2 and 7 showed relative increases in cell growth as compared to the control, of 19% and 21%, respectively. The remainder of the significant data for the 100µg/mL dilution showed relative decreases ranging from 6-21% (Figure 24). Cotinine is the primary metabolite of nicotine, as much as 80% of nicotine entering the body is metabolized to cotinine via the CYP2A6 complex. Next to nicotine, it is the most highly

studied alkaloid found in tobacco. Cotinine is able to exist in biological fluids much longer than nicotine (CDC), which may be partially responsible for the persistent effect seen in these growth assays, and the relative lack of an effect found in nicotine. It is possible that the relative increase seen in day 2 is the result of an initial stress response and the relative growth suppression in the following days is due to a relative depletion of resources and energy from said response. The increase seen in day 7 could be due to the control group reaching confluence earlier than the treated cells and beginning decay earlier, so the treated cells' growth curve would be shifted right in respect to the control curve. Though this effect would need to be subtle, because there is no dramatic shift of growth curves seen in the data.

The 1µg/mL dilution of the cotinine stock (1mg/mL) showed generally decreased growth compared to the control, with the exception of day 4, which was significant at α=0.05 and showed a 4.53% increase relative to the control (Figure 24). All data were significant at α=0.05, with the exception of days 5 and 7. Day 5 showed no significant difference, and day 7 showed a 21.9% decrease that was significant at α=0.1. Despite the increase on day 4 the rest of the data were decreased in relation to the control. This suggests that cotinine has an oppressive or dysregulatory effect on cell growth even at low concentrations.

The 100µg/mL dilution of the myosmine stock (1mg/mL) showed variances in growth that were significant at α=0.05 for all days with the exception of day 5, which was not significantly different from the control. Days 2, 6, and 7 all showed increased growth relative for the control by 28%, 13.5%, and 53.9%, respectively (Figure 24). The

explanation for this phenomena may be similar to that seen in cotinine, in which the initial spurt of growth was due to a strong stress response in the earlier days, followed by decreased growth due to lack of nutrients and energy. The increased growth seen during days 6 and 7 could be due to the growth curve of the treated cells being shifted subtly right in relation to the control curve.

The 1µg/mL dilution of the myosmine stock (1mg/mL) showed a lesser effect than the cotinine solution. Day 4 showed a small increase that was different from the control with a significance of $p<0.1$. Day 6 showed an increase of 11.6% in relation to the control, which was significant at $\alpha=0.05$ (Figure 24). In general, the growth curve for the 1µg/mL dilution closely mimics the control curve, suggesting only a mild effect at this low of a concentration.

The 100µg/mL dilution of the anabasine stock showed significant differences at days 3, 5, and 6. Days 3 and 5 were decreased in relation to the control by 30.7% and 17.3%, respectively. Day 6 was increased with respect to the control by 13.2% (Figure 24). The decrease seen in days 3 and 5 suggests a strong initial effect on growth, though without the initial growth surge on day 2 that was seen in the 100µg/mL dilutions of the other three alkaloids. Perhaps anabasine activates an alternative stress pathway than the other alkaloids. Increased growth on day 6 could be signs of cellular recovery, or shifts in the growth curve as hypothesized with the other alkaloids.

The 1µg/mL dilution of anabasine showed statistically significant differences on days 3, 5, and 6, as well as a difference that was significant at $\alpha=0.1$ for day 7. All significant differences were decreases in relation to the control by 19.6%, 14.8%, 16.8%

and 24.5%, respectively (Figure 24). This data suggests that even low concentrations of anabasine may have a significant effect on cell growth, over a relatively lengthy time period.

Differential Gene Expression in Response to Alkaloid Exposure

Alkaloid Effects on CX3CL1

Table 4: Gene Expression Data for CX3CL1. Units are in Normalized Fold Differences. N/A represents data that was below the limit of detection

CX3CL1 Expression				
	Nic	Myo	Ana	Cot
CTRL D2	0.43	1.47	0.44	N/A
100µg/mL D2	0.68	1.45	1.63	0.91
1µg/mL D2	6.05	N/A	1.82	1.27
CTRL D7	1.49	N/A	0.56	0.28
100µg/mL D7	1.25	0.94	1.08	1.05
1µg/mL D7	0.67	0.35	0.66	0.53

*Table 5: Representation of the percent difference in CEACAM6 expression between experimental conditions and control, for each alkaloid. ** Denotes p<0.05, * denotes p<0.1. N/A denotes values that were below the limit of detection..*

CX3CL1 Percent Difference				
	Nic	**Myo**	**Ana**	**Cot**
100µg/mL D2	59.61	-1.49%	268.46%	N/A
1µg/mL D2	1315.23%	N/A	312.89%	N/A
100µg/mL D7	-15.89%**	N/A	92.86%	272.37%
1µg/mL D7	-54.81%**	N/A	17.99%	86.88%

Table 6: P-Values generated using a type 2, two tailed student T-Test. N/A represents data that was unable to be generated due to replicates that were below the limits of detection.

CX3CL1 P-Values		
	Day 2	**Day 7**
Nic 100µg/mL	N/A	0.031
Nic 1µg/mL	N/A	0.26
Myo 100µg/mL	N/A	N/A
Myo 1µg/mL	N/A	N/A
Ana 100µg/mL	N/A	N/A
Ana 1µg/mL	N/A	N/A
Cot 100µg/mL	N/A	0.27
Cot 1µg/mL	N/A	0.738

.

The chemokine, CX3CL1, was very lowly expressed in our lung carcinoma cell line, CCL-185. The Bio-Rad IQ5 was sensitive enough to generate expression data for the majority of the conditions, with the several notable exceptions: myosmine 1µg/mL Day 2, myosmine CTRL Day 7, and cotinine CTRL Day 2 (Table 4). In the absence of the controls for myosmine day 7, and cotinine day 2 there is no baseline of comparison for the experimental conditions on these time points, and percent difference data can't be made (Table 5). Percent difference data was generated for the entirety of the nicotine and anabasine treated cultures, for both time points (Table 4). We were unable to perform t-tests on the majority of the data (Table 6), due to many of the replicates for each experimental condition being below the limit of detection, therefore rendering much of the data unreliable.

CX3CL1 is a chemokine, and chemoattractant signaling molecule, which plays a major role in immunity, cell migration, and inflammation. CX3CL1 promotes carcinogenesis by maintaining inflammation, and subsequently causing increased cell proliferation, which in an atmosphere like that of chronic inflammation may lead to increased probabilities of mutation and cancer cell formation. CX3CL1 also promotes

angiogenesis, which allows tumors to grow and their cells to divide with greater efficiency (Li *et al*, 2010). It is possible that the expression of *CX3CL1* would be more pronounced in a primary cell culture, in which these metabolic, and potentially carcinogenic changes were occurring, as opposed to in a cancer cell line in which these changes have already occurred. It would be difficult to generate data regarding angiogenesis, though there have been studies that utilized 3D cultures containing spheroids of tumor cells and endothelial cells which show endothelial tubule formation sustained by the tumor cells, with no external growth factors (Seano *et al*, 2013).

In the future, the issue of low expression may be ameliorated by increasing the amount of RNA in the cDNA conversion reaction, or by adding a greater amount of cDNA template to the RT-PCR reaction. This should not alter the results, because the experimental wells are compared to controls which reside on the same plate, and will have the same amount of cDNA or RNA in the reaction. Thus, the increase should be proportional throughout all wells, and adding more template will only cause an increase in detectable gene product.

Alkaloid Effects on SLIT1

Table 7: Gene Expression Data for SLIT1. Units are in Normalized Fold Differences. N/A represents data that was below the limit of detection.

SLIT1 Expression				
	Nic	Myo	Ana	Cot
CTRL D2	0.098	0.14	0.11	0.14
100µg/mL D2	0.0069	0.82	0.015	0.63
1µg/mL D2	N/A	0.36	0.22	0.44
CTRL D7	0.58	0.26	0.29	0.68
100µg/mL D7	0.27	1.24	0.67	1.15
1µg/mL D7	0.86	1.18	0.096	0.47

*Table 8: Representation of the percent difference in CEACAM6 expression between experimental conditions and control, for each alkaloid. ** Denotes p<0.05, * denotes p<0.1. N/A denotes values that were below the limit of detection*

SLIT1 Percent Difference				
	Nic	**Myo**	**Ana**	**Cot**
100µg/mL D2	-93.05	501.61	-85.89	353.34
1µg/mL D2	N/A	160.81	105.11	216.27
100µg/mL D7	-53.23	370.30**	127.95	68.99
1µg/mL D7	49.54	347.52**	-67.22	-30.52

Table 9: P-Values generated using a type 2, two tailed student T-Test. N/A represents data that was unable to be generated due to replicates that were below the limits of detection.

SLIT1 P-Values		
	Day 2	**Day 7**
Nic 100µg/mL	0.012518	0.385294
Nic 1µg/mL	N/A	0.429312
Myo 100µg/mL	N/A	0.017509**
Myo 1µg/mL	N/A	0.001586**
Ana 100µg/mL	N/A	0.56683
Ana 1µg/mL	N/A	0.809402
Cot 100µg/mL	N/A	0.597122
Cot 1µg/mL	0.723695	0.530542

SLIT1, a molecule involved in the complex processes of axonal guidance and angiogenesis, showed low normalized expression (Table 7). Percent differences between experimental conditions and controls were created using expression data (Table 8). Some p-values were generated from the cycle threshold data, however, many of these data were below the LOD and the p-values generated are based on incomplete replicates, and therefore are not reliable (Table 9).

This low expression may be explained by tissue localization of the SLIT1 protein. SLIT1 is a SLIT isoform that is mainly localized to neural tissue (Dickinson *et al*, 2004), and we utilized a lung cell culture for our experiments. SLIT1 also regulates highly complex, multi-tissue interactions, such as angiogenesis or neural guidance, and the simplistic nature of a 2D cell culture does not allow for these complex interactions to

occur, which may not elicit expression of SLIT1. Further attempts to determine expression of this gene could utilize higher quantities of RNA or cDNA template.

Alkaloid Effects on CEACAM6

*Table 10: Representation of the percent difference in CEACAM6 expression between experimental conditions and control, for each alkaloid. ** Denotes p<0.05, * denotes p<0.1.*

CEACAM6 Percent Difference				
	Nic	**Myo**	**Ana**	**Cot**
100µg/mL D2	87.81%*	35.55%**	-13.69%	-40.54%**
1µg/mL D2	168.2%**	23.09%**	-3.61%	-9.59%
100µg/mL D7	547.22%**	187.38**	-58.50%**	-7.51%
1µg/mL D7	407.37%**	220.26%	52.24%**	-30.92%**

Nicotine

The expression of *CEACAM6*, an adhesion molecule that is implicated in carcinogenesis and metastasis, was significantly ($p<0.05$) upregulated for the 1µg/mL dilution on day 2, as well as the 100µg/mL and 1µg/mL nicotine dilutions on day 7. The 100µg/mL nicotine dilution on day 2 showed upregulation of gene expression, that was marginally significant based on a $p<0.1$ (Table 10). CEACAM6 expression is inversely correlated to cellular differentiation (Blumenthal *et al*, 2007), so we would expect a higher baseline level in a non-transformative cancer cell line, such as CCL-185, though we did not compare expression levels between this cell line and a primary culture. The consistent upregulation of gene expression in response to even low levels of nicotine is consistent with research demonstrating that smokers have higher levels of *CEACAM6* mRNA than non-smokers (Spira *et al*, 2004). Though the cell line may have a higher baseline expression of *CEACAM6* than a primary cell source, we can use the increased

expression compared to the control cell culture as predictive to how a primary culture would respond to the same nicotine stimulus.

Myosmine

The expression of *CEACAM6* was significantly ($p<0.05$) upregulated for all dilutions and time points, with the exception of the 1µg/mL dilution on day 7 (Table 10). Myosmine's metabolism has been shown to have genotoxic effects, leading to carcinogenesis and tumorigenesis (Glas *et al*, 2007; Vogt *et al*, 2006). Upregulation of *CEACAM6* gene expression in response to myosmine may be associated with decreased cellular differentiation (Blumenthal *et al*, 2007), and increased metastatic capabilities (Ordoñez *et al*, 2000). The magnitude of *CEACAM6* gene expression showed a significant increase between Day 2 and Day 7, which may suggest that the mutagenic effects of myosmine increased over the week long time span, as opposed to cells showing recovery by the end of the week.

Anabasine

CEACAM6 showed significantly ($p<0.05$) decreased expression for the 100µg/mL anabasine dilution on the day 7 time-point, and significant upregulation of gene expression for the 1µg/mL anabasine dilution on the day 7 time-point. Both dilutions of the day 2 time-point showed reduced expression, but the values were not significant when $\alpha=0.05$ or $\alpha=0.1$ (Table 10). CEACAM6, aside from having implications in carcinogenesis and metastasis, also plays a role in phagocytosis of bacteria and viruses (Chapin *et al*, 2012). A recent study demonstrated decreased bacterial clearance as a result of lowered phagocytic capabilities in mice exposed to e-cigarette vapor (Sussan *et*

al, 2015). The effects of anabasine on immunity are not well documented, but anabasine's presence in e-cigarette refill solutions implicates it as a suspect for this decreased innate immunity. The increased expression of *CEACAM6* seen in the lower dilution of anabasine on the day 7 time-point may be explained by a dose-dependent mechanism for anabasine's inhibition of *CEACAM6*. Perhaps at the 1µg/mL dilution, over a period of seven days, the effects of CEACAM6 are able to overcome the downregulatory effects of anabasine.

Cotinine

CEACAM6 showed significantly ($p<0.05$) decreased expression resulting from exposure to the 100µg/mL dilution on day 2 (Table 10). The 1µg/mL dilution on day 7 showed decreased expression that was significant ($p<0.05$). Reduced expression of *CEACAM6* may indicate decreased immune function (Chapin *et al*, 2012), or increased tissue permeability due to weakened adherence to neighboring cells. Cotinine has been shown to decrease innate immunity by inhibiting the action of Toll Like Receptors (TLRs), prominent pattern recognition receptors associated with the innate immune system (Bagaitkar *et al*, 2012), and perhaps the decreased expression of *CEACAM6* is a function of decreased immunity.

Alkaloid Effects on ALDH3A1

*Table 11: Representation of the percent difference in ALDH3A1 expression between experimental conditions and control, for each alkaloid. ** Denotes p<0.05, * denotes p<0.1.*

ALDH3A1 Percent Difference				
	Nic	**Myo**	**Ana**	**Cot**
100µg/mL D2	4.20%	125.52%**	21.27%**	0.788%
1µg/mL D2	194.10%**	132.27%**	6.86%	27.55%*
100µg/mL D7	144.46%**	10.82%	64.98%**	50.52%**
1µg/mL D7	105.26%**	30.17%	82.01%**	-14.90%

Nicotine

ALDH3A1, a protein involved in the detoxification of reactive aldehydes during drug metabolism, showed significant upregulation for the 1µg/mL dilution on day 2, and the 100µg/mL and 1µg/mL nicotine dilutions on day 7. The 100µg/mL dilution for day 2 showed upregulation, but not at a level that was statistically significant at α=0.05 or α=0.1 (Table 11). Nicotine has been shown to induce oxidative stress in cell cultures (Crowley-Weber *et al*, 2003), which may increase reactive aldehyde species in serum or media. ALDH3A1 is an inducible aldehyde dehydrogenase isoform (Lindahl, 1992), and may therefore its expression may by increased as a result of increased oxidative stress, as is suggested by the data. Our results are consistent with previous experiments showing increased *ALDH3A1* expression in cell cultures exposed to cigarette smoke extract (Jang *et al*, 2014), as well as in the airways of smokers as compared to non-smokers (Spira *et al*, 2004).

Myosmine

ALDH3A1 showed significantly ($p<0.05$) increased expression for both myosmine dilutions on the day 2 time-point. ALDH3A1 showed upregulation of gene expression for

both myosmine dilutions of the day 7 time-point, but not at a level that was significant at α=0.05 or α=0.1 (Table 11). Myosmine, and its metabolites, have been shown to induce oxidative stress in mouse models (Simeonova *et al*, 2012). Increased *ALDH3A1* expression may be induced by increased oxidative stress resulting from myosmine exposure. The day 7 time-point showed only slight upregulation of gene expression compared to the control, which may indicate a degree of recovery. It is possible that the initial upregulation of *ALDH3A1*, and likely other genes responsible for fighting oxidative stress, were successful and were able to inactivate the oxidative stressors and return to normal levels by the day 7 time-point.

Anabasine

ALDH3A1 showed significantly ($p<0.05$) increased expression in response to the 100µg/mL dilutions of anabasine for both time points, as well as the 1µg/mL dilution on the day 7 time-point (Table 11). E-cigarette vapor exposure causes increased oxidative stress *in vivo* in mice, especially over long periods over exposure (i.e 2 weeks) (Chapin *et al*, 2015), which may be related to the observed increase in the magnitude of expression between the day 2 and day 7 time-points in the data. Nicotine and myosmine have both been shown to increase oxidative stress (Crowley-Weber *et al*, 2003; Simeonova *et al*, 2012), and based on the structural similarities between anabasine and the aforementioned alkaloids it is possible that anabasine may have a role in oxidative stress. The effects of anabasine on oxidative stress are poorly documented, but based on our data, the apparent induction of *ALDH3A1* expression during the later time period implicates anabasine in the production of oxidative stress. Interestingly, the pattern of *ALDH3A1* expression in response to anabasine opposes that of myosmine-induced expression, in which there was

a strong initial increase in expression, which eventually settled to near normal levels. Perhaps anabasine and its metabolites produce a lesser amount of oxidative stressors, thus only mildly activating the antioxidant response element, but as these stressors accumulate over the week-long time period they cause a more robust antioxidant response.

Cotinine

ALDH3A1 showed significantly ($p<0.05$) increased expression for the 100µg/mL dilution of cotinine on day 7, and only a mildly significant ($p<0.1$) upregulation of gene expression for the 1µg/mL dilution on day 2 (Table 11). Cotinine, a primary metabolite of nicotine, has been shown to induce the production of harmful oxidants and increased oxidative stress (Soto-Otero *et al*, 2002). This could cause the initial induction of the antioxidant, ALDH3A1. The decreased expression, though not deemed statistically significant though the triplicates for this time point are relatively close to one another (SD=0.019), seen in the 1µg/mL (Day 7) data may be due to the ability for ALDH3A1, and other antioxidant gene products, to overcome the oxidative stress produced by a low dilution of cotinine over a week long time period.

Alkaloid Effects on PIR

*Table 12: Representation of the percent difference in PIR expression between experimental conditions and control, for each alkaloid. ** Denotes p<0.05, * denotes p<0.1.*

PIR Percent Difference				
	Nic	**Myo**	**Ana**	**Cot**
100µg/mL D2	-32.01%*	6.63%**	-11.28%	-35.41%**
1µg/mL D2	-9.89%	22.49%**	-1.42%**	-22.19%
100µg/mL D7	-1.77%**	36.63%**	100.31%**	11.59%**
1µg/mL Day7	-6.51**	-15.76%**	-4.997%**	21.32%**

Nicotine

PIR, an important transcriptional regulator which has implications in apoptosis and oxidative stress response due to its relationship with NF-κB, showed significant ($p<0.05$) downregulation of gene expression for the 100µg/mL nicotine dilution and the 1µg/mL dilution on the day 7 time-point. The 100µg/mL dilution on the day 2 time-point showed downregulation with a $p<0.1$ (Table 12). Our findings are inconsistent with other research, which shows increased expression of *PIR* in response to oxidative stress and cigarette smoke (Gelbman *et al*, 2007). There are several aspects of this study which may cause this discrepancy. PIR is also upregulated and has a role in inducing apoptosis (Orsaez *et al*, 2001), likely by inhibiting the effects of the anti-apoptotic transcription factor NF-κB (Gelbman *et al*, 2007). This study utilized a continuous cancer cell line, which may have impaired apoptotic mechanisms and not express genes in this pathway in the same way as a primary culture. This study only examined these alkaloids in isolation, as opposed to the complex mixtures of chemicals associated with cigarette smoke or e-cigarette vapors, thus nicotine in isolation may not have an upregulating effect on *PIR* gene expression. Nicotine has also been shown to have anti-apoptotic properties by stimulating NF- κB activity (Tsurutani *et al*, 2005; Crowley-Weber *et al*, 2003), which may override the NF- κB inhibitory effects of PIR.

Myosmine

PIR showed significant ($p<0.05$) upregulation of gene expression for all day 2 dilutions, and the 100µg/mL dilution of myosmine on day 7. *PIR* showed significantly reduced expression for the 1µg/mL dilution on the day 7 time-point (Table 12).

Myosmine has been shown to induce cytostasis (halting the cell growth cycle) and apoptosis in cell cultures (Boteva *et al*, 2011), which may occur through a pathway regulated by PIR, a known contributor to apoptosis (Gelbman *et al*, 2007). The reason for the decreased expression associated with the 1µg/mL dilution on the day 7 time-point is unclear. Perhaps the negative effects related to a low concentration were not enough to overwhelm the cells, and the effects causing the induction of *PIR* expression seen in the same dilution on the day 2 time-point may have been ameliorated by the day 7 time-point.

Anabasine

PIR showed significant ($p<0.05$) downregulation of gene expression for the 1µg/mL anabasine dilution for both the day 2 and the day 7 time-points. However, the gene expression of *PIR* was significantly upregulated for the 100µg/mL dilution on the day 7 time-point (Table 12). *PIR* expression is upregulated during periods of oxidative stress and apoptosis (Gelbman *et al*, 2007; Orsaez *et al*, 2001). The increase in *PIR* expression at the 100µg/mL dilution on the day 7 time-point may be reflective of the same cause that potentially increased *ALDH3A1* expression for the same time point, an accumulation of oxidative stressors. Increased amounts of oxidative stress may cause increased expression of *PIR*, as suggested by previous literature (Gelbman *et al*, 2007). The downregulation of gene expression seen during the day 2 time-point and the 1µg/mL dilution on the day 7 time-point may be reflective of anti-apoptotic capabilities similar to that of nicotine, though research regarding anabasine's effect on apoptosis is minimal.

Alternatively, there may be less oxidative stress in the earlier time points and at lower dilutions.

Cotinine

PIR showed significant ($p<0.05$) differential expression for all time points and all dilutions of cotinine, with the exception of the 1µg/mL dilution on day 2. The 100µg/mL dilution on day 2 showed significantly reduced expression. Both dilutions showed significant upregulation of gene expression during the day 7 time-points (Table 12). Cotinine has been shown to promote lung tumorigenesis by activating the PI3K/Akt pathway, which is linked to apoptotic inhibition and cellular proliferation (Nakada *et al*, 2012). This pathway has also shown cross-talk with the NF-κB pathway, which also mediates an anti-apoptotic response. PIR has shown putative inhibitory behavior on the NF-κB transcription factor, and promotes apoptosis through this mechanism (Orsaez *et al*, 2000). The initial anti-apoptotic response induced by cotinine may be responsible for the decreased expression seen during the day 2 time-period. The increased expression seen in the later time period (Day 7) may be associated with a certain degree of recovery from the initial anti-apoptotic effects of cotinine, or may be associated with increased oxidative stress in these time points, which would be associated with increases in *PIR* expression (Gelbman *et al*, 2007).

Alkaloid Effects on TLR4

*Table 13: Representation of the percent difference in TLR4 expression between experimental conditions and control, for each alkaloid. ** Denotes p<0.05, * denotes p<0.1.*

TLR4 Percent Difference				
	Nic	**Myo**	**Ana**	**Cot**
100µg/mL D2	85.68%	-53.00%	-53.73%	-18.99%
1µg/mL D2	843.62%**	-45.24%	-26.16%	-64.83%
100µg/mL D7	3.57%	107.87%	-50.74%	-48.31%
1µg/mL D7	4.03%	142.28%	23.08%	-34.30%

Nicotine

TLR4, an important receptor of the innate immune system, showed upregulation of gene exression at all time-points and nicotine dilutions, though only the 1µg/mL dilution on day 2 showed upregulation that was statistically significant ($p<0.05$) (Table 13). TLR4 is largely known as a pattern recognition receptor (PRR) that associates with the endotoxic lipopolysaccharide present on the outer membrane of gram negative bacteria, but that is also present in pollution and smoke. Nicotine has been shown to induce respiratory inflammation through a TLR4 associated pathway, so it would not be surprising to see upregulation of gene expression in response to nicotine exposure (Lin *et al*, 2010). The large increase in expression that was deemed significant for the 1µg/mL dilution on day 2, may be due to the role of TLR4 as a receptor. It is possible that a low dilution of nicotine may allow the receptor to perform at a greater efficiency, while a higher concentration may cause the receptor to become saturated.

Myosmine

TLR4 showed decreased expression for both myosmine dilutions on the day 2 time-point, and it showed upregulation for both dilutions of the day 7 time-point (Table 13). No values for the myosmine dilutions were deemed statistically significant. Myosmine's effects on immunity are not well documented, so the root cause for the initial downregulation of gene expression is unclear. Cigarette smokers have been shown to have decreased innate immunity (Chen *et al*, 2007), and it is possible that myosmine contributes to this by decreasing the amount of TLR4 present on the surface of innate immune cells.

Anabasine

TLR4 showed downregulation of gene expression for the both dilutions on the day 2 time-point as well as the 100µg/mL dilution for the day 7 time-point, and upregulation for the 1µg/mL dilution on the Day 7 time-point. These data were not significant at α=0.05 or α=0.1 (Table 13). Interestingly, the data for the differential expression of *TLR4* in cells exposed to anabasine follows a similar pattern to the expression of *CEACAM6* when exposed to the same conditions. Both genes and their products have roles in innate immunity. The decreased expression of *TLR4* may lend further support to the aforementioned idea that anabasine plays a role in decreased innate immune response that is seen in smokers and e-cig users (Chen *et al*, 2007; Sussan *et al*, 2015). The upregulation of gene expression seen for the 1µg/mL dilution on the day 7 time-point, though not deemed statistically significant, may suggest that TLR4 is not greatly hindered by the low dilution over a period of seven days, or perhaps that the function of TLR4 as a receptor is more efficient at a low concentration.

Cotinine

TLR4 showed decreased gene expression for all dilutions of cotinine and time points, though none of them were deemed statistically significant at $\alpha=0.05$ or $\alpha=0.1$ (Table 13). Based on previous literature, we would expect to see decreased *TLR4* expression in response to cotinine exposure (Bagaitkar *et al*, 2012). Bagaitkar and colleagues showed downregulation of ligand-stimulated TLR4 and a decrease in the downstream pro-inflammatory cytokine response, due to levels of cotinine exposure that are physiologically relevant to smokers.

Limitations

This is a pilot study, based on our funding, resources and time. A 2D culture system as a model for complex physiological processes does not necessarily mimic the human response properly (Abbot, 2003; Weaver *et al*, 1997). Cultures grown in 3D suspensions, such as hydrogel matrices, or in the extracellular matrix of the tissue being studied have been shown to be more physiologically accurate (Weaver *et al*, 1997). We also utilized a continuous carcinoma cell line, which is likely to have differential gene expression in comparison to healthy tissues. In the future we would like to utilize primary cultures in these experiments, as they would provide a more accurate of an e-cigarettes effect on healthy cells and genomic changes.

We used a liquid media to expose the cell cultures to the primary alkaloids, when in reality these alkaloids would be aerosolized. There have been experiments which use machines to produce aerosols of these extracts (Trehy *et al*¸2011; Jensen *et al*, 2015). This would produce effects that are more true to actual e-cigarette exposure, however we

do not have the resources required to purchase or create one of these machines. However, the experiments conducted within these limitations are still useful to better understand how these chemicals interact with living cells *in vitro*.

Table 14: Characteristics of the Failed Primers

Gene	Sequence 5'-3'	Tm°C	Product Length	PCR Efficiency
CYP1A1 (a). FP	CCCAACCCTTCCCTGAATG	62.2	146	N/A
CYP1A1 (a). RP	TTCTCCTGACAGTGCTCAATC	61.8		
CYP1A1 (b). FP	TCATTGTAACTCAGAGACCACTAAC	62.2	137	N/A
CYP1A1 (b). RP	CATTATGGCAGGAAAAGGGTTG	61.9		
CYP1A1 (c). FP	ACAGATGCTTTGGTCTTTTATGC	62.0	150	N/A
CYP1A1 (c). RP	AGGATTTAATGCCCAGTGTAGC	62.6		
AHR. FP	CCACATCACCTACGCCAG	62.3	135	N/A
AHR. RP	CCAAACGGTCCAACTCTGTAT	62.1		

We were unable to study all of the genes listed in the proposal. Several of the primers were unable to show specificity for their gene products (Table 14), such as CYP1A1, AHR, and GPX2. Several of the genes had to be examined multiple times using qRT-PCRs. At several points the cell cultures became unhealthy and would not adhere to the tissue culture flasks, which required us to restart the cultures from frozen reserves. It became difficult to grow and isolate enough cells to produce a meaningful quantity of RNA to be converted to cDNA. Cell cultures will be maintained and more cDNA will be produced, and these genes will be studied following my DHON defense. I plan to continue working on this project into the summer, and I will help Dr. Kovach train another student to continue this project into the future.

Conclusion

Cell viability studies, utilizing the Cell-titer Glo ATP Luminescent Assay, showed generally decreased cell viability, or cell proliferation, in cell cultures exposed to the individual alkaloids found in e-cigarette refill solutions: nicotine, myosmine, anabasine, and cotinine. The examination of differential gene expression, using qRT-PCR, showed significant differential expression for each gene and each alkaloid being examined in this study. Two of the genes, *SLIT1* and *CX3CL1*, showed expression which was below the limit of detection (LOD) for the methods of examination we utilized, which suggests that these genes and their products are not highly expressed in lung tissue, or that the cancer cell line, CCL-185, does not highly express these genes. *TLR4* showed differential expression in response to all alkaloids, but did not show statistical significance for these differences, which may be a result of procedural or human error and may be alleviated with repetition. Each of these genes serves a particular function in the cell: adhesion (*CEACAM6, CX3CL1*), immune response (*TLR4, CX3CL1, CEACAM6*), xenobiotic metabolism (*CYP1A1, AHR, ALDH3A1*), oxidative stress (*GPX2, ALDH3A1*), putative oncogenes (*PIR, CEACAM6*), or putative tumor suppressor genes (*SLIT1*). Differential expression of these genes has been implicated in carcinogenesis and tumorigenesis. Overall, the differential expression observed in this study was variable depending on the alkaloid and time point (Table 14), and thus were not unanimously consistent with the predictions made in the hypothesis (Table 1; Table 14). Certain alkaloids showed expected patterns of gene expression, for instance, *ALDH3A1* showed increased expression for each alkaloid, as predicted in the hypothesis. This being said, differential

expression, either increased or decreased, for any of these genes may be associated with a potentially deleterious response within the cell, or within the body as a whole.

Table 15. Observed Differences in Gene Expression for Candidate Genes

Gene	ALDH3A1	CEACAM6	PIR	TLR4
Predicted Expression	Increased	Increased	Increased	Decreased
Observed Expression	Generally increased as a result of exposure to each alkaloid	Increased for myosmine and nicotine; decreased for anabasine and cotinine	Nicotine and anabasine were reduced. Myosmine was increased. Cotinine was reduced for D2 and increased for D7.	Nicotine showed increased expression. Cotinine and anabasine were reduced. Myosmine was reduced for D2 and increased for D7.

The differential expression, as well as the decreased cell viability, seen in our study suggests an insidious nature of these chemicals in regards to human health, and should inspire further investigation into the physiological effects of e-cigarettes, as well as the standards of regulation that apply to the marketing and labeling of e-cigarette products.

Future Directions

The experiments outlined in this thesis will need to be repeated to ensure validity of the measurements, and allow us to reduce the effects of random and procedural error. Considering the growth curves peaked at day 5, we would like to investigate gene expression on this day during future experiments. This project investigated gene expression on a transcript level, it would be interesting to investigate protein expression of the genes being studied, because mRNA expression has not always been shown to have a strong correlation with corresponding protein expression (Guo *et al*, 2008), though

the correlation is seen to be stronger in differentially expressed mRNA (Koussanadis *et al,* 2015). We would like to perform western blots of the genes being studied in order to study varied protein expression. This would allow us to see if the differential expression seen on the transcript level carried over onto the translational level. Protein expression may also be examined qualitatively using immunohistochemical (IHC) or immunofluorescent (IF) staining of the proteins in question. This would allow us to examine the localization and distribution of the various proteins, while the western blotting would allow a more quantitative view of the protein expression. Immunofluorescent stains may be visualized using fluorescent microscopy or laser confocal microscopy, both of which are assets possessed by UTC. Both western blots and staining would likely utilize the same antibodies targeted for the protein being studied, which would be financially advantageous.

Cell viability assays and RT-PCR will be carried out on combinations of the alkaloids being studied, which will allow us to examine how the physiology changes when presented with more complex solutions, like those that are actually found in the refill cartridges. It will allow us to determine if the alkaloids will have compounding effects, or if one alkaloid, or combination of alkaloids, may ameliorate the changes produced by another. Experiments examining transcript expression and cell viability will also be carried out in cells exposed to commercially available e-cigarette refill solutions. It would also be beneficial to develop a way to expose the cells to aerosols of the various alkaloids and refill solutions, as this is how these chemicals are introduced *in vivo*, therefore experimentation using this method may convey a more accurate representation of the physiological responses occurring in e-cigarette users.

This experimental protocol should also be repeated utilizing a primary cell line, as opposed to a cancer cell line. A primary cell line would allow a closer examination of how normal cell physiology changes in response to e-cigarette refill solutions, and may better show morphological and genetic changes associated with carcinogenesis and tumorigenesis.

The field of e-cigarette research is still burgeoning, though more information is coming out rapidly as lab groups shift their focus to what is now becoming a global trend. This project is providing a pivot point for e-cigarette research, switching from quantitative examination of the chemical components to examination of how these components affect human and cellular physiology. As more data of this nature is accrued, it will become more clear how e-cigarettes affect human health on not only the individual scale, but on the scale of public health. Research of this nature will provide a basis for future laws and regulations regarding e-cigarettes, and allow for a more informed generation of e-cigarette users.

Work Cited

Abbot A (2003) Cell Culture: Biology's New Dimension. *Nature* 424(6951): 870-872.

Abdollahi A, Schwager C, Kleeff J, Esposito I, Domhan S, Peschke P, Hauser K, Hahnfeldt P, Debus J, Peters JM, Friess H, Folkman J, Huber P (2007) Transcriptional Network Governing the Angiogenic Switch in Human Pancreatic Cancer. *PNAS* 104(31): 12890-12895.

Allen JG, Flanigan SS, LeBlanc M, Vallarino J, MacNaughton P, Stewart JH, Christiani DC (2015) Flavoring Chemicals in E-Cigarettes: Diacetyl, 2,3-Pentanedione and Acetoin in a Sample of 51 Products, Including Fruit-, Candy-, and Cocktail-Flavored E-Cigarettes. *Environ Health Perspect*; DOI:10.1289/ehp.1510185

Antilla S, Vainio H, Hietan E, Camus AM, Malaveille C, Brun G, Husgafvel-Pursiainen K, Heikkila L, Karjalainen A, Bartsch H (1992) Immunohistochemical Detection of Pulmonary Cytochrome P4501A and Metabolic Activities Associated with P450IA1 and P450IA2 Isozymes in Lung cancer Patients. *Env Health Persp* 98: 179-182.

Anroutsopoulos V, Tsatsakis AM, Spandidos DA (2009) Cytochrome P450 CYP1A1: Wider Roles in Cancer Progression and Prevention. *BMC Cancer* 9(1): 187.

Armstrong DW, Wang X, Lee JT, Lie YS (1999) Enantiomeric Composition of Nornicotine, Anatabine, and Anabasine in Tobacco. *Chirality* 11(1): 82-84.

Avci ME, Konu O, Yagci T (2008) Quantification of SLIT-ROBO Transcripts in Hepatocellular Carcinoma Reveals Two groups of Genes with Coordinate Expression. *BMC Cancer* 8: 392-403.

Bagaitkar J, Zeller I, Renaud DE, Scott DA (2012) Cotinine Inhibits the Pro-inflammatory Response Initiated by Multiple Cell Surface Toll-Like Receptors in Monocytic THP Cells. *Tob Induc Dis* 10(1): 18.

Bahl V, Lin S, Xu N, Davis B, Wang Y, Talbot P (2012) Comparison of Electronic Cigarette

Refill Fluid Cytotoxicity Using Embryonic and Adult Models. *Repro Tech* 34(4): 529-537.

Beavers, C (2014) The Effects of E-Cigarettes on Cell Growth. BS Departmental Honors Thesis, University of Tennessee Chattanooga.

Benowitz NL (1996) Cotinine as a Biomarker of Environmental Tobacco Smoke Exposure. *Epidemiological Rev* 18(2): 188-204.

Benowitz NL (2008) Clinical Pharmacology of Nicotine: Implications for Understanding, Preventing, and Treating Tobacco Addiction. *Clin Pharm & Therap* 83(4): 531-541.

Benowitz NL, Hukkanen J, Jacob P (2009) Nicotine Chemistry, Metabolism, Kinetics and Biomarkers. *Handb Exp Pharmacol* (192): 29-60.

Black W, Chen Y, Matsumoto A, Thompson DC, Lassen N, Pappa A, Vasiliou V (2012) Molecular Mechanisms of ALDH3A1-mediated Cellular Protection Against 4-hydroxy-2-nonenal. *Free Rad Bio and Med* 52(9): 1937-1944.

Blumenthal RD, Leon E, Hansen HJ, Goldenberg DM (2007) Expression Patterns of CEACAM5 and CEACAM6 in Primary and Metastatic Cancers. *BMC Cancer* 7: 2-17.

Brauze D, Fijalkiewicz K, Szaumkessel M, Kiwerska K, Bednarek K, Rydzanicz M, Richter J, Grenman R, Jarmuz-Szymczak M (2014) Diversified Expression of

Aryl Hydrocarbon Receptor Dependent Genes in Human Laryngeal Squamous Cell Carcinoma Cell Lines Treated with β-naphthoflavone. *Tox Lett* 231: 99-107.

Boyle JO, Gumus ZH, Kacker A, Choksi VL, Bocker JM, Zhou XK, Yantiss RK, Hughes DB, Du B, Judson BL, Subbaramiah K, Dannenberg AJ (2010) Effects of Cigarette Smoke on the Human Oral Mucosa Transcriptome. *Cancer Prev Res* 3(3) 266-278.

Borsig L, Wolf MJ, Roblek M, Lorentzen A, Heikenwalder M (2014) Inflammatory Chemokines and Metastasis-Tracing the Accessory. *Oncogene* 33(25): 3217-3224.

Boteva BI, Mateva RM, Iliev IA, Gorneva GA (2011) Flow Cytometry Analysis of the Influence of Myosmine on the Cell Cycle. *Croatia Chemica Acta* 84(3): 355-359.

Callahan Lyon P (2014) Electronic Cigarettes: Human Health Effects. *Tob Cont* 23(Suppl 2): ii36-ii40.

Caponnetto P, Campagna D, Papale G, Russo C, Polosa R (2012) The Emerging Phenomenon of Electronic Cigarettes. *Expert Rev Respir Med* 6(1): 63-74.

Carroll-Chapman S, Wu L (2014) E-Cigarette Prevalence and Correlates of Use Among Adolescents Versus Adults: A Review and Comparison. *J Psychiatr Res* 54: 43-54.

Chapin C, Bailey NA, Gonzales LW, Lee J, Gonzales RF, Ballard PL (2012) Distribution and Surfactant Association of Carcinoembryonic Cell Adhesion Molecule 6 in Human Lung. *Am J Physiol Lung Cell Mol Physiol* 302(2): 216-225.

Chatham-Stephens K, Law R, Taylor E, Melstrom P, Bunell R, Wang B, Apelberg B, Schier JG (2014) Notes From the Field: Calls to Poison Centers for Exposures to Electronic Cigarettes-United States, September 2010-February 2014. *CDC MMWR* 63(13): 292-293.

Chen H, Cowan MJ, Hasday JD, Vogel SN, Medvedev AE (2007) Tobacco Smoking Inhibits Expression of Proinflammatory Cytokines and Activation of IL-1R-Assiciated Kinase, p38, and NF-kappaB in Alveolar Macrophages Stimulated with TLR2 and TLR4 Agonists. *J Immunol* 179(9): 6097-6106.

Chen Z, Li Z, Niu X, Ye C, Yu Y, Lu S, Chen Z (2011) The Effect of CYP1A1 Polymorphisms on the Risk of Lung Cancer: A Global Meta-Analysis Based on 71 Case-Control Studies. *Mutagenesis* 26(3): 437-446.

Clemens KJ, Caille S, Stinus L, Cador M (2009) The Addition of Five Minor Tobacco Alkaloids Increases Nicotine Induced Hyperactivity, Sensitization and Intravenous Self-Administration in Rats. *Int Jour of Neuropsychopharmacology* 12(10): 1355-1366.

Crooks PA, Dwoskin LP (1997) Contribution of CNS Nicotine Metabolites to the Neuropharmacological Effects of Nicotine and Tobacco Smoking. *Biochem Pharma* 54(7): 743-753.

Crowley-Weber CL, Dvorakova K, Crowley C, Bernstein H, Bernstein C, Garewal H, Payne CM (2003) Nicotine Increases Oxidative Stress, Activates NF-κB and GRO78, Induces Apoptosis and Sensitizes Cells to Genotoxic/Xenobiotic Stresses by a Multiple Stress Inducer, Deoxycholate: Relevance to Colon Carcinogenesis. *Chem-Biological Interactions* 145(1): 53-66.

Dani JA, De Biasi M (2001) Cellular Mechanisms of Nicotine Addiction. *Pharma Biochem and Behavior* 70(4): 439-446.

Dasgupta P, Rizwani W, Pillai S, Kinkade R, Kovacs M, Rastogi S, Banerjee S, Carless M, Kim E, Coppola D, Haura E, Chellappan S (2009) Nicotine Induces Cell Proliferation, Invasion and Epithelial-Mesenchymal Transition in a Variety of Human Cancer Cell Lines. *Int Jour of Cancer* 124(1): 36-45.

Dickinson RE, Dallol A, Bieche I, Krex D, Morton D, Maher ER, Latif F (2004) Epigenetic Inactivation of SLIT3 and SLIT1 Genes in Human Cancers. *Brit Journ of Cancer* 91(12): 2071-2078.

Eisenberg E, Levanon EY (2013) Human Housekeeping Genes, Revisited. *Cell Press* 29(10): 569-574.

Farsalinos KE, Spyrou A, Stefapoulos C, Tsimopoulou K, Panagiota K, Tsiapras D, Kyrzopoulos S, Poulas K, Voudris V (2015) Nicotine Absorption from Electronic Cigarette Use: Comparison between Experienced Consumers (Vapers) and Naïve Users (Smokers).*Sci Reports* 5: doi:10.1038/srep11269

FDA (2009) Laboratory Analysis of Electronic Cigarettes Conducted by FDA. http://www.fda.gov/NewsEvents/PublicHealthFocus/ucm173146.htm

Fraga D, Meulia T, Fenster S (2008) Real-Time PCR. *Current Protocols Essential Laboratory Techniques*. Unit 10.3.

Gelbman BD, Heguy A, O'Connor TP, Zabner J, Crystal RG (2007) Upregulation of Pirin Expression By Chronic Cigarette Smoking is Associated with Bronchial Epithelial Cell Apoptosis. *Respir Res* 8(1): 10.

Glas S, Tyroller S, Zwickenpflug W, Steiner K, Kiefer G, Richter E (2007) Tissue Distribution and Excretion of Myosmine After IV Administration to Long-Evans Rats Using Quantitative Whole-Body Autoradiography. *Arch Toxicol* 81: 151-161.

Goniewicz ML, Lee L (2015) Electronic Cigarettes are a Source of Thirdhand Exposure to Nicotine. *Nic & Tobacco Res* 17(2): 256-258.

Gori GB, Benowitz NL, Lynch CJ (1986) Mouth Versus Deep Airways Absorption of Nicotine in Cigarette Smokers. *Pharm Biochem and Behavior* 25(6): 1181-1184.

Guo Y, Xiao P, Lei S, Deng F, Xiao GG, Liu Y, Chen X, Li L, Wu S, Chen Y, Jiang H, Tan L, Xie J, Zhu X, Liang S, Deng H (2008) How is mRNA Expression Predictive for Protein Expression? A Correlation Study on Human Circulating Monocytes. *Acta Biochimica Et Biophysica Sinica* 40(5): 426-436.

Harris AC, Tally L, Muelken P, Banal A, Schmidt CE, Cao Q, LeSage MG (2015) Effects of Nicotine and Minor Tobacco Alkaloids on Intracranial-Self-Stimulation in rats. *Drug and Alc Dependence* 153: 330-334.

Hatsukami D, Lexau B, Nelson D, Pentel PR, Sofuoglu M, Goldman A (1998) Effects of Cotinine on Cigarette Self-Administration. *Psychopharmacology* 138: 184-189.

Hukkanen J, Jacob P, Benowitz NL (2005) Metabolism and Disposition Kinetics of Nicotine. *Pharm Rev* 57(1): 79-115.

Jang J, Bruse S, Liu Y, Duffy V, Zhang C, Oyamada N, Randell S, Matsumoto A, Thompson DC, Lin Y, Vasiliou V, Tesfaigzi Y, Nyunoya T (2014) Aldehyde Dehydrogenase 3A1 Protects Airway Epithelial Cells from Cigarette Smoke-Induced DNA Damage and Cytotoxicity. *Free Rad Bio and Med* 68: 80-86.

Jensen RP, Luo W, Pankow JF, Strongin JF, Peyton DH (2015) Hidden Formaldehyde in E-Cigarette Aerosols. *NEJM* 372(4): 392-394.

Kim KS, Kim J, Lee S, Kang MA, Choe IS, Kang YH, Kim S, Yeom YI, Lee Y, Kim JH, Kim KH, Kim CN, Kim JW, NamM, Lee HG (2013) Overexpression and Clinical Significance of Carcinoembryonic Antigen-Related Cellular Adhesion Molecule 6 in Colorectal Cancer. *Clinica Chimica Acta* 415: 12-19.

Klein K, Winter S, Turpeinen M, Schwab M, Zanger UM (2010) Pathway Targeted Pharmacogenomics of CYP1A2 in Human Liver. *Pharmacogenetics and Pharmacogenomics* 1(129): 1-20.

Komai K, Niwa Y, Sasazawa Y, Simizu S (2015) Pirin Regulates Epithelial to Mesenchymal Transition Independent of Bcl3-Slug Signaling. *FEBS Lett* 589(6): 738-743.

Korkalainen MK, Torronen AR, Karenlampi SO (1995) Comparison of Expression of Aldehyde Dehydrogenase 3 and CYP1A1 in Dominant and Recessive Aryl Hydrocarbon Hydroxylase-Deficient Mutant Mouse Hepatoma Cells. *Chemico-Biological Interactions* 94(2): 121-134.

Koussounadis A, Langdon SP, Um IH, Harrison DJ, Smith VA (2015) Relationship Between Differentially Expressed mRNA and mRNA-protein Correlations in a Xenograft Model System. *Sci Rep* 5: 10775.

Kozlowski LT, Mehta NY, Sweeney CT, Schwartz SS, Vogler GP, Jarvis MJ, West RJ (1998) Filter Ventilation and Nicotine Content of Tobacco in Cigarettes From Canada, The United Kingdom, and the United States. *Tob Cont* 7(4): 396-375.

Lee ST, Wildeboer K, Panter KE, Kem WR, Gardner DR, Molyneux RJ, Chang CT, Soti F, Pfister JA (2006) Relative Toxicities and Neuromuscular Nicotinic Receptor Agonistic Potencies of Anabasine Enantiomers and Anabaseine. *Neurotox and Teratology* 28(2): 220-228.

Li F, Wang Z, Liu Y, Li J (2010) Down-Regulation of Fraktalkine Inhibits the In Vitro and In Vivo Angiogenesis of the Hepatocellular Carcinoma HepG2 Cells. *Oncol Rep* 24(3): 669-675.

Lin CC, Lee I, Yang Y, Lee C, Kou YR, Yang C (2010) Induction of the COX-2/PGE2/IL-6 is Crucial for Cigarette Smoke Extract-Induced Airway Inflammation: Role of TLR4-Dependent NADPH Oxidase Activation. *Free Rad Bio and Med* 48(2): 240-254.

Lindahl R (1992) Aldehyde Dehydrogenases and Their Role in Carcinogenesis. *Crit Rev in Biochem and Molec Bio* 27(4-5): 283-335.

Liu F, Rehmani I, Esaki S, Fu R, Chen L, Serrano V, Liu A (2013) Pirin is an Iron-dependent Redox Regulator of NF-κB. *PNAS* 110(24): 9722-9727.

Livak KJ, Schmittgen TD (2001) Analysis of Relative Gene Expression Data Using Real-Time Quantitative PCR and 2-ΔΔCT Method. *Methods* 25(4): 402-408.

McBride JS, Altman DG, Klein M, White W (1998) Green Tobacco Sickness. *Tob Cont* 7(3): 294-298.

Mehlen P, Delloye-Bourgeois C, Chedotal A (2011) Nover Roles for SLITS and Netrins: Axon Guidance Cues as Anticancer Targets? *Nat Rev Cancer* 11(3): 188-197.

Miyazaki I, Simizu S, Okumura H, Takagi S, Osada H (2010) A Small-Molecule Inhibitor Shows that Pirin Regulates Migration of Melanoma Cells. *Nat Chem Bio* 6(9): 667-673.

Murray JL (2014) Nicotine and What Else?: HPLC Elution Optimization for the Analysis of Alkaloids Found in Electronic Cigarettes. BS Departmental Honors Thesis, University of Tennessee Chattanooga.

Nakada T, Kiyotani K, Iwano S, Uno T, Yokahira M, Yamakawa K, Fujieda M, Saito T, Yamazaki H, Imaida K, Kamataki T (2012) Lung tumorigenesis Promoted by Anti-Apoptotic Effects of Cotinine, a Nicotine Metabolite Through Activation of PI3K/Akt Pathway. *Jour of Tox Sciences* 37(3): 555-563.

Ordoñez C, Screaton RA, Ilantzis C, Stanners CP (2000) Human Carcinoembryonic Antigen Functions as a General Inhibitor of Anoikis. *Cancer Res* 60(13): 3419-3424.

Orsaez D, de Jong AJ, Woltering EJ (2001) A tomato Homologue of the Human Protein PIRIN is Induced During Programmed Cell Death. *Plant Mol Bio* 46: 459-468.

Schober W, Szendrei K, Matzen W, Osiander-Fuchs H, Heitmann D, Schettgen T, Jorres RA, Fromme H (2014) Use of Electronic Cigarettes (e-cigarettes) Impairs Indoor Air Quality and Increases FeNO Levels of E-Cigarette Consumers. *Int J of Hygiene and Env Health* 217(6): 628-637.

Seano G, Chiaverina G, Gagliardi PA, di Blasio L, Sessa R, Bussolino F, Primo L (2013) Modeling Human Tumor Angiogenesis in a Three-Dimensional Culture System. *Blood* 121(21): 129-137.

Simeonova R, Vitcheva V, Galina G, Mitcheva M (2012) Effects of Myosmine on Antioxidative Defense in Rat Liver. *Arch Indust Hygiene & Tox* 63(1): 7-14.

Singh A, Rangasamy T, Thimmulappa RK, Lee H, Osburn WO, Brigelius-Flohe R, Kensler TW, Yamamoto M, Biswal S (2006) Glutathione Peroxidase 2, the Major Cigarette Smoke-Inducible Isoform of GPX in Lungs, Is Regulated by Nrf2. *Am J Respir Cell Mol Bio* 35(6): 639-650.

Soto-Otero R, Mendez-Alvarez E, Hermida-Ameijeiras A, Lopez-Real AM, Landeira-Garcia JL (2002) Effects of (-)-Nicotine and (-)-Cotinine on 6-hydroxydopamine-induced Oxidative Stress and Neurotoxicity: Relevance for Parkinson's Disease.

Spira A, Beane J, Shah V, Liu G, Schembri F, Yang X, Palma J, Brody JS (2004) Effects of Cigarette Smoke on the Human Airway Epithelial Cell Transcriptome. *PNAS* 101(27): 10143-10148.

Stark R, Choi H, Koch S, Lamb F, Sherwood E (2015) Monophosphoryl Lipid A Inhibits the Cytokine Response of Endothelial Cells Challenged with LPS. *Inn Immun* 21(6): 565-574.

Sussan TE, Gajghate S, Thimmulappa RK, Ma J, Kim JH, Sudini K, Consolini N, Cormier SA, Lomnicki S, Hasan F, Pekosz A, Biswal S (2015) Exposure to Electronic Cigarettes Impairs Pulmonary Anti-bacterial and Anti-Viral Defenses in Mouse Model. *PLoS One* 10(2).

Taghavi S, Khashyarmanesh Z, Moalemzadeh-Haghighi H, Nassirli H, Eshraghi P, Jalali N, Hassanzzadeh-Khayyay M (2012) Nicotine Content of Domestic Cigarettes, Imported Cigarettes and Pipe Tobacco in Iran. *Addiction & Health* 4(1-2): 28-32.

Trehy ML, Wei Y, Hadwiger ME, Moore TW, Allgire JF, Woodruff JT, Ahadi SS, Black JC, Westenberger BJ (2011) Analysis of Electronic Cigarette Cartridges, Refill Solutions, and Smoke for Nicotine and Nicotine Related Impurities. *J of Liq Chrom & Rel Tech* 34(14): 1442-1458.

Tsurutani J, Castillo SS, Brognard J, Granville CA, Zhang C, Gills JJ, Sayyah J, Dennis PA (2005) Tobacco Components Stimulate Akt-dependent Proliferation and NFκB-dependent Survival in Lung Cancer Cells. *Carcinogenesis* 26(7): 1182-1195.

Vogt S, Fuchs K, Richter E (2006) Genotoxic Effects of Myosmine in a Human Esophageal Adenocarcinoma Cell Line. *Toxicology* 222(1-2): 71-79.

Weaver VM, Peterson OW, Wang F, Larabell CA, Briand P, Damsky C, Bissel MJ (1997) Reversion of the Malignant Phenotype of Human Breast Cells in Three-Dimensional Culture and In Vivo by Integrin Blocking Antibodies. *Jour Cell Bio* 137(1): 231-245.

Wu G, Fang Y, Yang S, Lupton JR, Turner ND (2004) Glutathione Metabolism and Its Implications for Health. *J Nutr* 134(3): 489-492.

Yildiz D (2004) Nicotine, Its Metabolism and an Overview of Its Biological Effects. *Toxicon* 43: 619-632.

Ypsilanti AR, Zagar Y, Chedotal A (2010) Moving Away From the Midline: New Developments for Slit and Robo. *Devo* 137(12): 1939-1952.

Yue B, Kushnir MM, Urry FM, Rockood AL (2010) Quantitation of Nicotine, its Metabolites, Other Related Alkaloids in Urine, Serum, and Plasma Using LC-MS-MS. *Methods in Molec Bio* 613: 389-398.